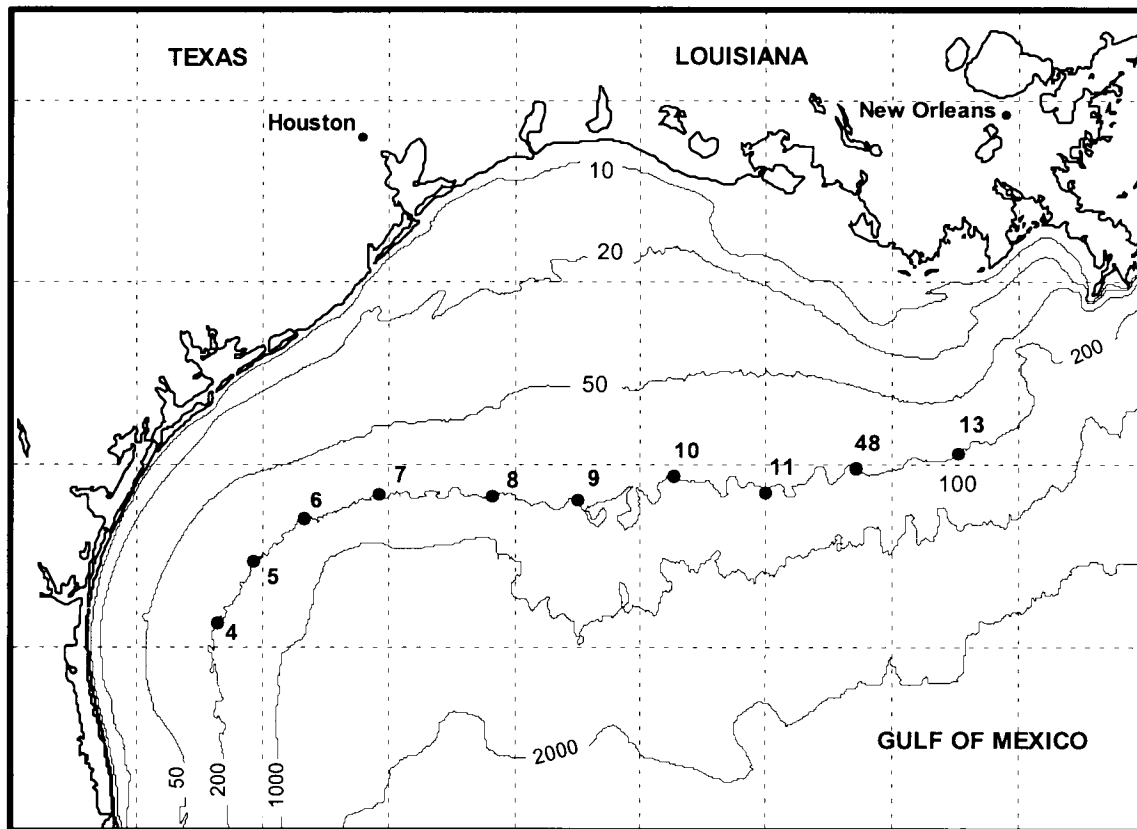




Coastal Marine Institute

Dynamic Height and Seawater Transport across the Louisiana-Texas Shelf Break

Final Report



Coastal Marine Institute

Dynamic Height and Seawater Transport across the Louisiana-Texas Shelf Break

Final Report

Authors

Carole L. Current
William J. Wiseman, Jr.

June 2000

Prepared under MMS Contract
14-35-0001-30660-19948
by
Coastal Marine Institute
Louisiana State University
Baton Rouge, Louisiana 70803

Published by

**U.S. Department of the Interior
Minerals Management Service
Gulf of Mexico OCS Region**

**Cooperative Agreement
Coastal Marine Institute
Louisiana State University**

DISCLAIMER

This report was prepared under contract between the Minerals Management Service (MMS) and the Coastal Studies Institute, Louisiana State University. This report has been technically reviewed by the MMS and approved for publication. Approval does not signify that the contents necessarily reflect the views and policies of the Service, nor does mention of trade names or commercial products constitute endorsement or recommendation for use. It is, however, exempt from review and compliance with MMS editorial standards.

REPORT AVAILABILITY

Extra copies of the report may be obtained from the Public Information Office (Mail Stop 5034) at the following address:

U.S. Department of the Interior
Minerals Management Service
Gulf of Mexico OCS Region
Public Information Office (MS 5034)
1201 Elmwood Park Boulevard
New Orleans, Louisiana 70123-2394

Telephone Number: 1-800-200-GULF or
504-736-2519

CITATION

Suggested citation:

Current, C. L. and W. J. Wiseman, Jr. 2000. Dynamic height and seawater transport across the Louisiana-Texas shelf break. OCS Study MMS 2000-045. U.S. Dept. of the Interior, Minerals Management Service, Gulf of Mexico OCS Region, New Orleans, LA. 46 pp.

ABOUT THE COVER

The cover art shows the Louisiana-Texas shelf and the locations of ten moorings at the shelf edge from which temperature and salinity data used to estimate cross-shelf transport in this study were collected.

TABLE OF CONTENTS

CHAPTER	PAGE
I. INTRODUCTION.....	1
1.1 Background.....	1
1.2 Overview of the Present Study.....	3
II. METHODS	5
2.1 Data and Data Products.....	5
2.2 Dynamic Vertical Structure Functions for Pressure Anomaly.....	6
2.2.1 Reference Profiles.....	8
2.2.2 Computation of Modes	9
2.3 Fit of Mooring Data to Dynamic Modes.....	10
2.4 Estimation of Dynamic Height and Geostrophic Transport.....	12
III. RESULTS	13
3.1 Modal Amplitudes Along the Louisiana-Texas Shelf Break	13
3.2 Dynamic Height.....	15
3.3 Transport Across the Louisiana-Texas Shelf Break.....	18
IV. DISCUSSION	25
V. SUMMARY AND CONCLUSIONS	29
LITERATURE CITED.....	31
APPENDIX A: VERTICAL PROFILES OF SHELFWIDE TRANSPORT	33
APPENDIX B: ESTIMATED TRANSPORT BY SHELF REGION	39

LIST OF FIGURES

Figure		Page
1	The positions of 10 LATEX-A shelf break moorings that provided salinity and temperature data from which time dependent pressure anomaly profiles, dynamic height, and geostrophic transport were estimated.	2
2	Typical CTD deployment patterns for LATEX-A hydrographic cruises (filled circles); above, full shelf; below, half shelf.	7
3	Seasonal mean hydrostatic stability profiles for the Louisiana-Texas shelf, with examples of seasonally fitted reference columns (thin lines) used for vertical dynamic mode computations. (a) fall-winter, (b) spring, and (c) summer.	9
4	Typical seasonal shelf-wide dynamic modes of pressure anomaly.	11
5	First and second baroclinic pressure anomaly mode amplitude coefficients B_n versus seafloor depth on the Louisiana-Texas shelf from LATEX-A cruise hydrography and from shelf break mooring data.	13
6	Monthly shelf-wide modal amplitude means for (a) barotropic, (b) first baroclinic, and (c) second baroclinic modes. Upstream (o) and downstream (x) modal amplitude means for (d) barotropic, (e) first baroclinic, and (f) second baroclinic modes.	16
7	Two component Fourier fit to seasonal steric water level averages computed from LATEX hydrographic cruise data (filled circles) at about 94°W near the 200-m isobath on the Louisiana-Texas continental shelf.	18
8	Mean offshore geostrophic transport per half meter depth across the Louisiana-Texas shelf break for (a) downcoast, (b) midshelf, and (c) upcoast Louisiana-Texas shelf break regions for time intervals treated in this study.	21
9	Seasonal average geostrophic transport per half meter depth in the offshore direction across the Louisiana-Texas shelf break.	22
A1	Shelfwide transports per half meter depth in the onshore direction across the Louisiana-Texas shelf break, 15-day means from April 21 – July 3, 1992.	35
A2	Shelfwide transports per half meter depth in the onshore direction across the Louisiana-Texas shelf break, 15-day means from September 26 - November 19, 1992.	36

Figure		Page
A3	Shelfwide transports per half meter depth in the onshore direction across the Louisiana-Texas shelf break, 15-day means from January 31 – May 5, 1993.	37
B1	Estimated offshore transport per km from April 28 – June 17, 1992, as a function of distance north and east along the 200-meter isobath from LATEX-A mooring 4.....	41
B2	Estimated offshore transport per km from October 3 – November 12, 1992, as a function of distance north and east along the 200-meter isobath from LATEX-A mooring 4.....	42
B3	Estimated offshore transport per km from February 7 – March 9, 1993, as a function of distance north and east along the 200-meter isobath from LATEX-A mooring 4.....	43
B4	Estimated offshore transport per km from March 19 – April 28, 1993, as a function of distance north and east along the 200-meter isobath from LATEX-A mooring 4.....	44
B5	Estimated offshore geostrophic transport across the Louisiana-Texas shelf break by alongshelf region. (a) April 28-June 27, 1992; (b) October 3 – November 12, 1992; and (c) February 7 – April 28, 1993.	45

LIST OF TABLES

Table		Page
1	Seasonal statistics of barotropic, first baroclinic, and second baroclinic mode amplitudes for 144 15-day mean pressure profiles on the Louisiana-Texas shelf break.....	15
2	Alongshelf regional statistics of modal amplitudes for 144 15-day mean pressure profiles on the Louisiana-Texas shelf break.....	17
3	Estimated transport (in Sverdrups) off the Louisiana-Texas shelf at the 200-meter isobath, listed by alongshelf region at specified depth ranges and days.....	19
4	Estimated transport (in Sverdrups) off the Louisiana-Texas shelf at the 200-meter isobath, listed by alongshelf region for the full water column and also listed for the entire shelf break at specified depth ranges.....	20
5	Mean seasonal offshore geostrophic transport at the Louisiana-Texas shelf break in Sverdrups ($10^6 \text{ m}^3/\text{s}$).	26
6	Monthly average direction of cross-shelf flow at the shelf break (200-meter isobath) for the present study and for the Bender study (in parentheses).	27

I. INTRODUCTION

1.1 Background

The transport of seawater onto and off of the Louisiana-Texas continental shelf is relevant to a broad variety of CMI and MMS interests in this region, where extensive offshore oil and gas production coexists with some of our nation's strongest and most productive fisheries. The present study is focused on the understanding and quantification of horizontal transport of seawater across the shelf break, as estimated by applying the assumption of geostrophy.

The Louisiana-Texas continental shelf extends nearly 1,000 km from the Rio Grande river mouth to Southwest Pass in eastern Louisiana. Although it is less than 90 km wide in the south, the midshelf region near Galveston and Sabine is broad with rough and irregular bottom features across more than 200 km width. The total volume of seawater on the shelf is roughly $8 \times 10^{12} \text{ m}^3$ at any given time. The shelf break is located at approximately the 200-m isobath (Figure 1). Cochrane and Kelly (1986) describe a seasonal pattern of circulation on the Louisiana-Texas shelf in which alongshelf flow on the inner shelf is downcoast (from Louisiana following the coastline south and west towards south Texas) except during the summer months, when it reverses and upcoast flow prevails. The outer shelf flow is upcoast (from south Texas north and east towards Louisiana) throughout the year. Cross-shelf flow is generally offshore in the south and onshore in the east, but this too reverses during the summer months. However the results of LATEX-A (Texas-Louisiana Shelf Circulation and Transport Processes Study) only partially confirmed the Cochrane and Kelly pattern of circulation, and were particularly equivocal on the outer Louisiana-Texas shelf. Alongshelf flow on the inner shelf is downcoast except for the summer months, and averages more than 0.25 Sv in the downcoast direction (Nowlin et al. 1998). It is not clear where this tremendous volume of water originates and how it leaves the shelf. The Mississippi-Atchafalaya River system delivers a mass flux of the order of 10% of the Louisiana-Texas shelf volume inside the 90-m isobath (Dinnel and Wiseman 1986). Additional mass flux to the shelf is delivered by excess rainfall, smaller rivers and eddy-shelf interactions. The timing, loci, and removal mechanisms of this water from the shelf in order to maintain a first order mass balance is an intriguing and complex oceanographic problem. This variable exchange carries with it a variety of dissolved and particulate materials, e.g. salt, nutrients, heat, sediments, larvae, and tar balls.

Bender and Reid determined transports across the Louisiana-Texas shelf break, as reported by Nowlin et al. (1998). Monthly averaged moored current meter velocity data were fitted to EOFs (empirical orthogonal functions) from 4 m deep by 10 km long binned ADCP (acoustic doppler current profiler) velocity data to estimate box model volume fluxes for each of 18 box sides. They concluded that the cross-shelf flux over the 200-m isobath is generally stronger than the outer shelf alongshelf fluxes and shows no discernible seasonal pattern. Bender and Reid did not focus on geostrophic flow alone, although current meter data along the shelf break contains a strong geostrophic flow component. Chen (1995) found that only about 30% of the variance in the LATEX-A ADCP data is ageostrophic, and about 70% is geostrophic. Other LATEX-A scientists carefully investigated the current meter record data using a variety of time-frequency

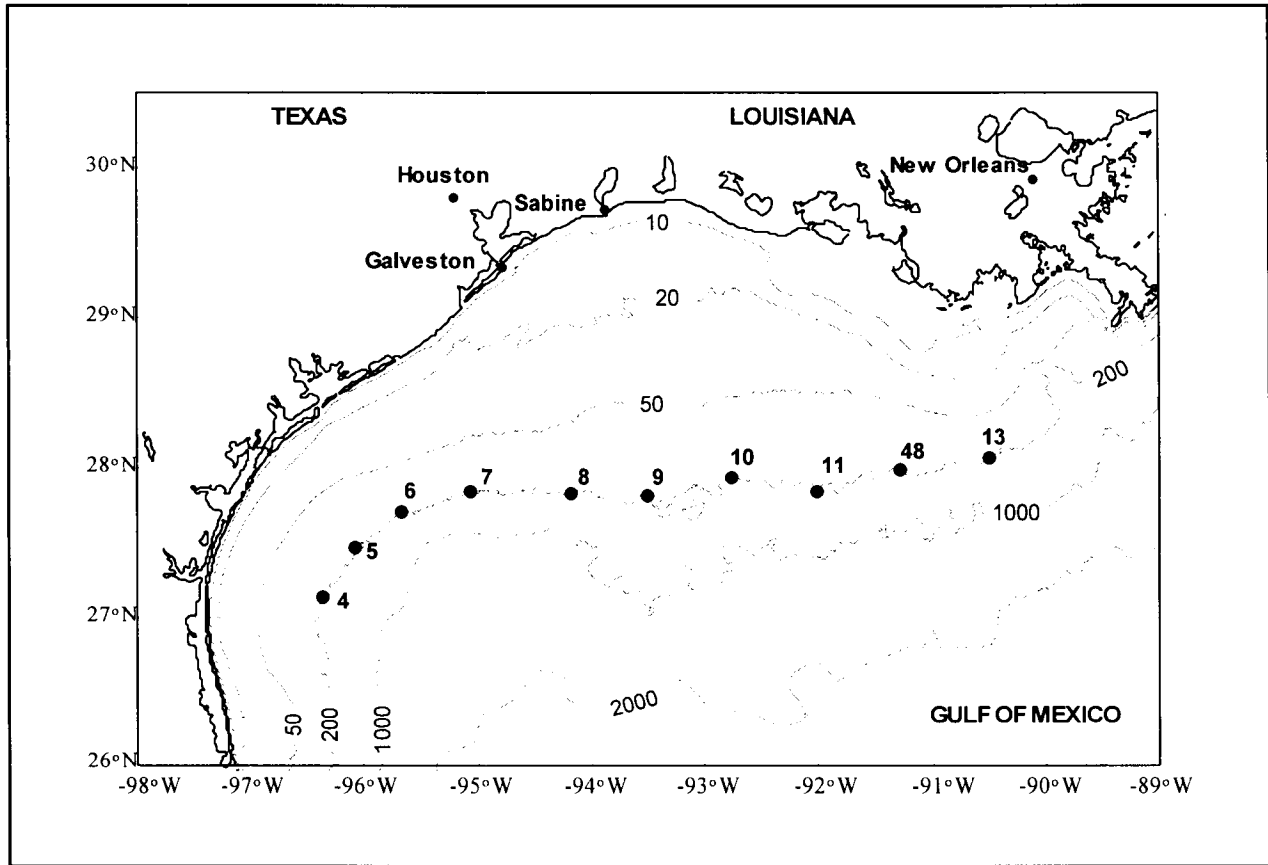


Figure 1. The positions of 10 LATEX-A shelf break moorings that provided salinity and temperature data from which time dependent pressure anomaly profiles, dynamic height, and geostrophic transport were estimated.

domain techniques in an attempt to identify free and forced waves and solitons, and seasonality of shelf break flow patterns. Results were of mixed success and these investigations are continuing.

The present study is confined to the shelf break region, employing a different methodology than that of Bender and Reid to estimate cross-shelf *geostrophic* transport. The dynamic structure functions used in this study are dependent on the long wave assumption as part of the linear dynamics used in their computation. Therefore, the use of these structure functions acts as a filter, screening out high frequency and nonlinear effects that can produce bias and inaccuracies in estimates of geostrophic transport. The use of hydrographic data on which to base our structure functions is also conducive to focus on geostrophic flow. The shape of a leveled state reference profile based on hydrographic data may be less prone to bias high frequency signal than is a reference based on ADCP data. For these reasons any overlap of this and the Bender and Reid calculations is complementary, and not a duplication of effort.

Our study quantifies time dependent, highly vertically resolved geostrophic transport of waters from the Gulf of Mexico across the Louisiana-Texas continental shelf break, and provides a first order picture of the spatial and temporal variability of shelf break exchange processes. Cross-shelf transport is large, and consistent with the findings of Bender and Reid. The annual volume of water transported off the shelf across the shelf break is approximately equal to the total volume of water on the shelf.

1.2 Overview of the Present Study

The present study begins with the determination of orthogonal patterns of pressure anomaly that are *characteristic of geostrophic flow*, computed from LATEX-A field hydrography and assumed dynamics of the system. Shelf break mooring data then is projected onto these patterns of variability, which are called dynamic vertical structure functions or dynamic modes (Kundu et al. 1975; Flierl 1978; SAIC 1989; Arango and Reid 1990; Current 1993). Estimates of time varying pressure anomaly profiles and dynamic height are produced by the summation of weighted dynamic modes, and estimation of cross-shelf geostrophic transport follows from these profiles by invoking geostrophic balance.

Computation of dynamic vertical structure functions requires a reference column, which is determined from hydrography. In order to seasonally adjust the structure functions for more efficient representation of the data, these structure functions are re-computed for each period during which data was collected, averaged, and fitted to them in the modal analysis using reference columns adjusted to that specific time of year. Density profiles from the hydrography are used to compute these smoothed, seasonally adjusted leveled state reference profiles. These reference columns are used in computing local dynamic vertical structure functions for pressure anomaly. The orthogonal patterns of variability are computed from the assumed dynamics of the system as well as the hydrographic profiles, and are highly resolved in the vertical.

The projection of mooring data onto these dynamic modes requires fitting the data at each mooring location, for each time step, to the dynamic structure functions in order to determine modal amplitudes. Time-dependent pressure anomaly information derived from measurements at individual top, middle, and bottom moorings were fitted to three local orthogonal dynamic modes by standard techniques to obtain modal amplitudes. High resolution pressure anomaly profile estimates were then reconstructed by summing the weighted modes at each mooring during each time step. Dynamic height anomalies were estimated using the Montgomery/Csanady method (Csanady 1979), and cross-shelf transport was estimated from an assumption of geostrophy and pressure anomaly profiles computed relative to a 250 meter reference depth.

II. METHODS

2.1 Data and Data Products

The recently completed LATEX-A program, sponsored by MMS, collected mooring and hydrographic data over the Louisiana-Texas continental shelf during the 32 months from April, 1992 through December, 1994. The best spatial and temporal coverage of this large data set is arguably in the vicinity of the shelf break. Current meter arrays with near surface, mid-depth, and near bottom meters, recorded velocity, temperature, and salinity at five minute intervals. These arrays were deployed at a spacing of no more than 90 km along the 200-m isobath between 90.5W and 27.1N. Furthermore, each of the hydrographic cruises collected CTD (conductivity-temperature-depth instrument) profiles along the 200-m isobath at a spacing of approximately 20 km.

Spatial correlation scales over the shelf were generally exceeded by separation distances between current meter mooring locations (Li et al. 1996). Despite these current meter separations, Cho et al. (1998) found reasonable patterns of shelf-wide monthly mean streamfunction using only near surface current meter data and standard analysis techniques. The moorings along the 200-m isobath were deployed in an especially closely spaced pattern that is favorable for the reliable estimation of dynamic height and cross-shelf transport, as in this study.

Moorings 4, 5, 6, 7, 8, 9, 10, 11, 48, and 13 deployed for LATEX-A were the source of hourly top (~14 meter), middle (~100 meter), and bottom (~190 meter) temperature and salinity time series used in this study. These 10 moorings were located along the 200-m isobath at the Louisiana-Texas shelf break as depicted in Figure 1. Data taken from these moorings were 40-hour low-passed, and density (σ_θ) time series were computed from temperature and salinity values using EOS-80 (Fofonoff 1985). Three extended time periods with uninterrupted top, middle, and bottom 40-hour low-passed values at most moorings were identified and selected as the focus of this study in order to maximize the degrees of freedom available for modal representation. Summer, fall, winter, and spring measurements were encompassed by this subset (April 20 – July 13, 1992, September 26 – November 25, 1992, and January 31 – May 7, 1993). Summer is defined as June through August, fall as September through November, winter as December through February, and spring as March through May, for the present study. Prior studies often have selected two seasons on this shelf, summer and non-summer. Summer data with uninterrupted top, middle, and bottom temperature and salinity series were sparse, however. By selecting four seasons, the spring and fall transition periods between winter and summer could be treated separately both for dynamic height and transport, and combined non-summer transports are discussed in Chapter 5. Mean densities were obtained for 15-day periods with five day overlaps, resulting in mean top, middle, and bottom densities at ten day intervals at each mooring. A first approximation of these time dependent σ_θ profiles was made by means of linear interpolation between top, middle, and bottom measurements and extension to the surface and to the seafloor. This extension was done by linear extrapolation of the trend between the middle and the top (or bottom) measurements to the surface (or seafloor). The mean 100 meter hourly σ_θ for all 10 moorings is at approximately mid-depth in the water column for these shelf break

moorings, and was taken to roughly represent a barotropic mean and was removed from all σ_θ values. The modal amplitudes are found relative to this estimated shelf *break* mean reference density (26.4 kg/m^3) in order to provide a realistic estimate of the barotropic vertical mode amplitudes of the local pressure anomaly profiles at the shelf break.

Pressure anomaly profiles were obtained following the method of Montgomery/Csanady (Csanady 1979). Pressure at 250 meters was taken to be 0.0 decibars with a corresponding σ_θ of 28.1 kg/m^3 , a mean value estimated by linear extrapolation using the mean σ_θ at the middle and bottom measurement depths, approximately 100 meters and 190 meters. The same 250 meter estimated σ_θ of 28.1 kg/m^3 was found by linear integration along each cross-shelf line of each LATEX-A hydrographic cruise by Current (1996). Pressures were then obtained, with respect to 250 meters, by integrating upwards through the water column employing the relation

$$P_j = P_{j-1} - g \left(\frac{\sigma_j + \sigma_{j-1}}{2} \right) (z_{j-1} - z_j) \quad (1)$$

The subscripts j and $(j-1)$ refer to the value at the present and next deepest level, respectively, at intervals of 0.5 meters in the 200-m water column, and σ is the σ_θ value adjusted as described.

Seasonal reference profiles and the dynamic vertical structure functions based on them were determined independently from CTD data collected on full shelf and half shelf hydrographic cruises (Figure 2). These hydrographic profiles were available digitally with measurements separated by only 0.5 meters depth, which allowed the computation of high resolution dynamic structure functions. Stability profiles were computed from the density profiles using the relation

$$N^2 = - \frac{g}{\rho} \frac{\partial \rho}{\partial z} \quad (2)$$

2.2 Dynamic Vertical Structure Functions for Pressure Anomaly

Hydrographic data were used to compute vertical dynamic structure functions that are based on seasonal shelf-wide reference columns of pressure anomaly and additional information provided by the assumed dynamics of the system. These structure functions are obtained by application of linear dynamics to a reference density profile, and have the advantage (in comparison with purely empirical structure functions such as EOF's) of screening out the effects of high frequency and nonlinear phenomena. Dynamic structure functions of this kind are particularly suited for use in the estimation of geostrophic transport.

Modal amplitudes of pressure anomaly were estimated by fitting the modes to pressure anomalies computed from mooring data. The resulting modal amplitudes then provide estimated pressure anomaly profiles at the mooring location to within 0.5 m of any depth, and were integrated from

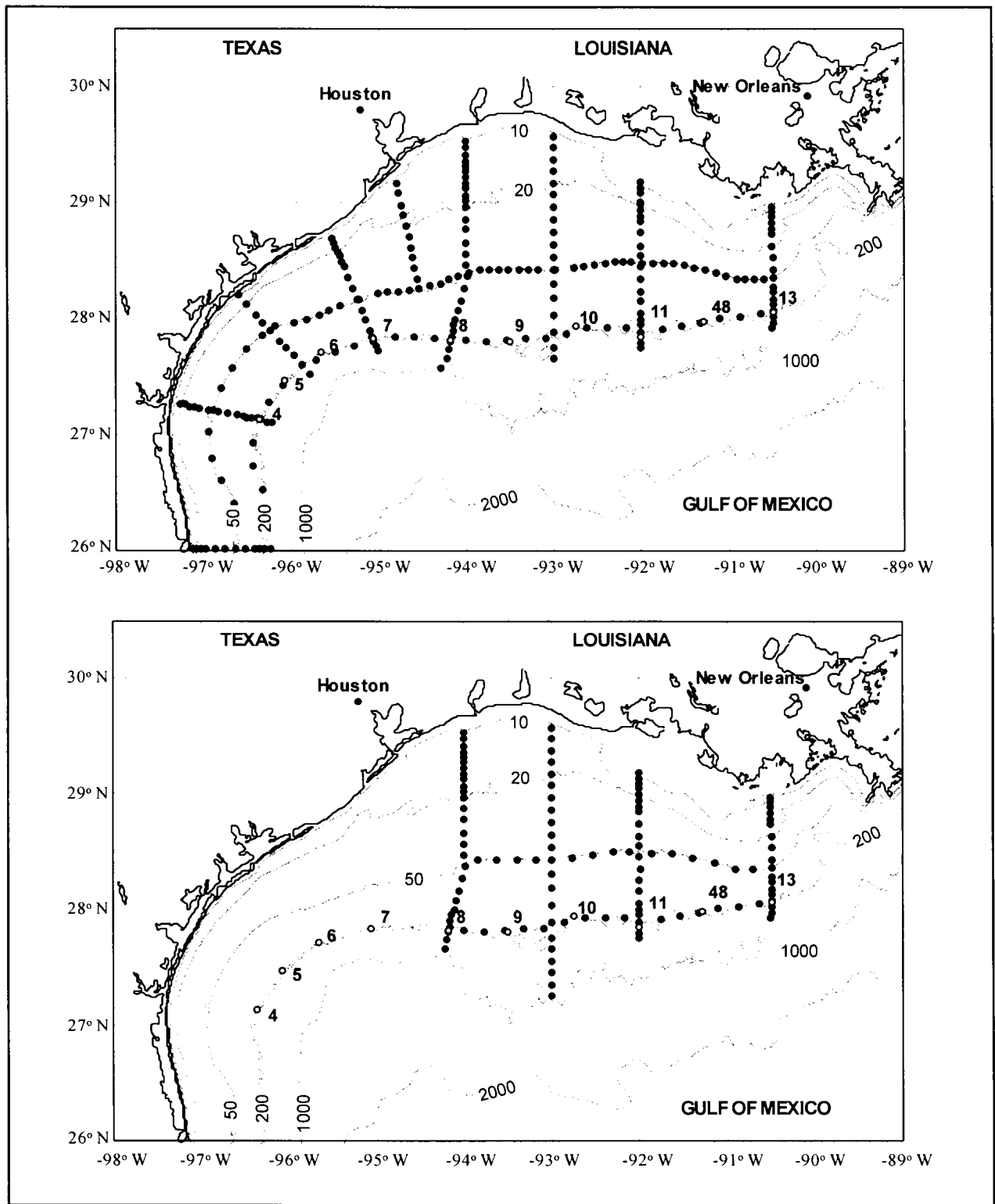


Figure 2. Typical CTD deployment patterns for LATEX-A hydrographic cruises (filled circles); above, full shelf; below, half shelf. Vertical dynamic modes were computed using seasonally adjusted mean profiles independently obtained from hydrographic data and fitted to time series from ten moorings (open circles).

surface to seafloor to obtain estimated dynamic height. High resolution estimates of depth dependent flow at the shelf break were then obtained by applying the assumption of geostrophic balance, and are potentially useful information not previously available to MMS. The focus on low frequency geostrophic cross-shelf transport in the absence of effects of tides and wind forcing in the weatherband is consistent with the smoothing of mooring data by time averaging over a 15 day period with five day overlap.

2.2.1 Reference Profiles

Seasonal shelf-wide reference columns of hydrostatic stability were fitted to LATEX-A hydrographic data, taking N^2 to be

$$N^2 = \begin{cases} N_o^2 + N_1^2 |z - z_c| & z > 70 \text{ m} \\ N_o^2 & z \leq 70 \text{ m} \end{cases} \quad (3)$$

where

$$N_o^2 = \exp(1.613 * 10^{-5} z^2 + 0.0197z + 5.7220) \quad (4)$$

and

$$N_1^2 = -103.9 + 239.5 \cos(\omega t) - 63.1 \sin(\omega t) + 64.4 \cos(2\omega t) \quad (5)$$

The second harmonic sine term was also computed but was found to be negligible. The phase (ωt) equals zero on the first day of August, following Current (1996). The variable ω is defined as the annual frequency, $2\pi/\text{year}$.

Mean stability profiles computed from corresponding hydrographic profiles using (2) are depicted in Figure 3 with examples of these seasonally fitted reference columns. Seasonal variability was allowed in the upper 70 meters of the water column. This depth was selected by subjective examination of residuals remaining from the hydrographic data for each season after the initial fit.

Local dynamic vertical modes of pressure anomaly were calculated with respect to these smoothed, seasonally adjusted leveled state reference profiles obtained independently from hydrographic cruise data. The use of a seasonal mean stability profile as a reference for computing structure functions allows these functions to represent only the variability, or signal, superimposed on this mean, and so improves the efficiency of representation of the data. The dynamic reference column is smoothed by superimposing the influence of seasonal variability (N_1^2) on a basic smooth, exponential stability profile (N_o^2) that does not vary with season. Seasonal effects are superimposed at water column depths not exceeding 70 meters. This is done by linear interpolation of the initial exponential stability profile above 70 m to Fourier fitted mean seasonal stabilities at the surface. Smoothed reference columns constructed by this method are depicted in Figure 3. The smoothing procedure removes irregularities in the mean profile. The resulting simplicity of representation improves computational efficiency.

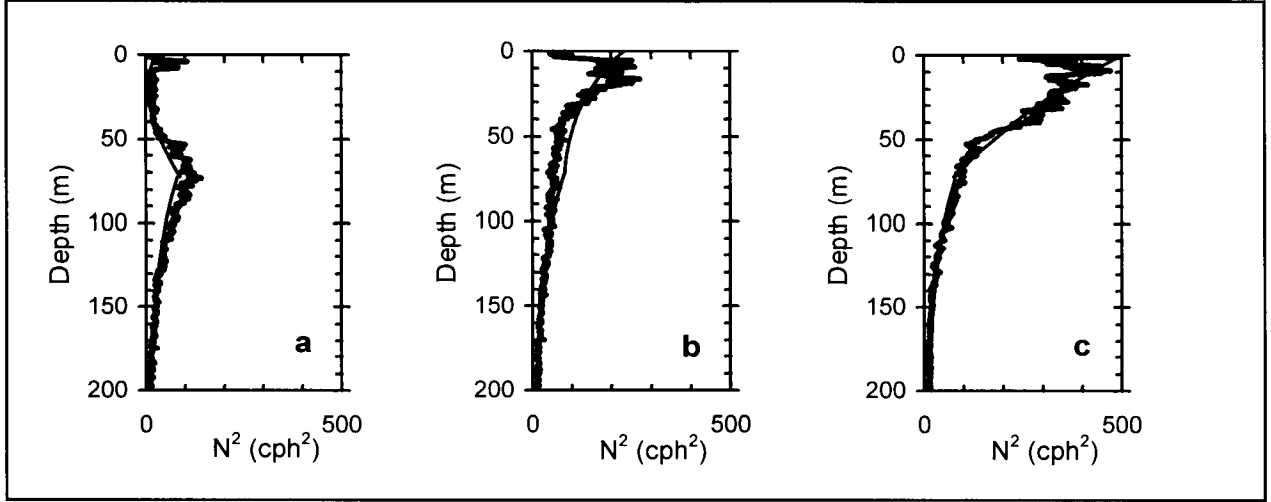


Figure 3. Seasonal mean hydrostatic stability profiles for the Louisiana-Texas shelf, with examples of seasonally fitted reference columns (thin lines) used for vertical dynamic mode computations. (a) fall-winter, (b) spring, and (c) summer.

2.2.2 Computation of Modes

The dynamic modes are orthogonal patterns of variability computed from the assumed dynamics of the system, providing added information based on physics to improve the resolution of estimated profiles obtained from measurements at a given time and location. These dynamic modes of pressure anomaly are rigid lid, flat bottom vertical structure functions based on the usual Sturm-Liouville boundary value problem arising from the equations of motion,

$$\frac{\partial}{\partial z} \left[\frac{1}{N^2} \frac{\partial F_n}{\partial z} \right] + \frac{1}{c_n^2} F_n = 0 \quad (6)$$

$$\frac{1}{N^2} \frac{\partial F_n}{\partial z} = 0 \quad \text{at } z = 0, h \quad (7)$$

Here F_n is the non-dimensional mode n structure function for kinematic pressure anomaly, N^2 is the rest state Brunt-Väisälä stability parameter, and c_n is the modal eigencelerity. The local structure functions F_n are orthonormalized.

The long wave approximation, which is necessary for the customary separation of variables, limits the usefulness of the analysis to the subinertial frequencies, but does not impede analyses such as the present study emphasizing low frequency phenomena.

The boundary value problem defined by (6) and (7) is developed from momentum and continuity equations under the hydrostatic approximation (i.e. negligible vertical acceleration).

The pressure anomaly modes were found relative to the dynamic reference column of Section 3.3, and are depicted in Figure 4 computed relative to typical summer, fall, winter, and spring reference columns. Similar local dynamic structure functions were computed for individual LATEX hydrographic stations in a pilot study for this project. These structure functions are reminiscent of the local vertical structure functions computed throughout the deep Gulf of Mexico by Current (1993), although the isopycnic coordinate system employed in that study is replaced here by a Cartesian coordinate system.

2.3 Fit of Mooring Data to Dynamic Modes

Time-varying amplitudes (B_n) of the local dynamic modes were estimated by individually fitting time dependent pressure anomaly from each of the 10 shelf break moorings to these orthogonal dynamic structure functions using

$$B_n = \frac{1}{h} \sum_{j=1}^J (p_{j-1} F_{n,j-1} + p_j F_{n,j}) \frac{(z_{j-1} - z_j)}{2}, \quad n = 0,1,2 \quad (8)$$

for each level j from surface to seafloor. Pressure anomalies were obtained from time dependent temperature and salinity measurements by means of relation (1), and linear methods were employed to estimate high resolution pressure anomaly (p) profiles and to extend these profiles throughout the entire water column. The mooring data analyzed were taken during times when measurements were available at all three instrument depths. The degrees of freedom present justify the use of no more than three dynamic modes during the periods analyzed. Therefore only the barotropic ($n = 0$), first baroclinic ($n = 1$), and second baroclinic ($n = 2$) mode amplitudes were estimated.

High resolution *reconstructed* profiles of pressure anomaly from sea surface to sea bed were obtained by employing the local vertical structure functions ($F_{n,j}$) and modal amplitudes (B_n) at each time step for each level j ,

$$p_j = \sum_{n=0}^2 B_n F_{n,j} \quad (9)$$

These time series of reconstructed pressure profiles are the basis for estimation of the time evolution of dynamic height and cross-shelf geostrophic transport at the 200-m isobath. Modal reconstruction of the data represented 97% of the variance in the data. Contributions of higher modes ($n = 3, 4, \dots, \infty$) and other possible causes for lack of fit (such as error in the estimation of pressure anomaly profiles) are included as residuals. These residuals are especially high during the month of June, and discussion of the contribution of higher modes to summer pressure anomaly can be found in Chapter 3.

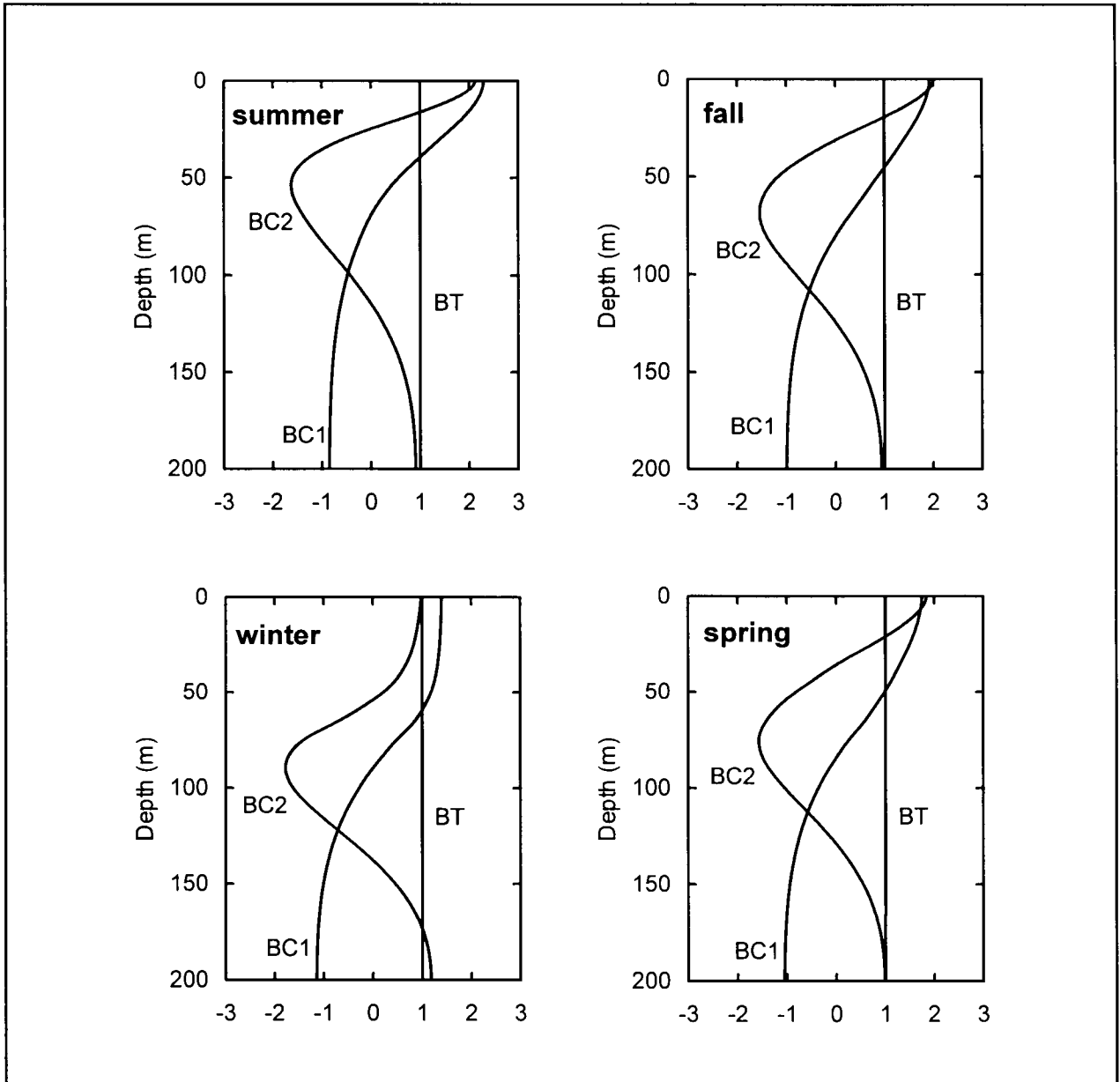


Figure 4. Typical seasonal shelf-wide dynamic modes of pressure anomaly.

Wind driving is known to influence alongshore currents on the Louisiana-Texas shelf (Cochrane and Kelly 1986), and wind driving is substantially associated with phenomena in the weatherband (two to ten day period) although longer periods become relatively more important during the summer. Because the focus of this study is on geostrophic flow of lower frequency, the present analysis was restricted to 15-day averages of density data with five day overlaps. Signal in the weatherband frequencies is not resolved by the present method.

2.4 Estimation of Dynamic Height and Geostrophic Transport

Time dependent dynamic heights were directly obtained from the high resolution pressure anomaly profiles using equation (1). Dynamic heights were then adjusted by removal of an annual mean estimated by equal weighting of seasonal means.

The cross-shelf geostrophic flow at the shelf break was estimated by applying the geostrophic balance to the high resolution reconstructed pressure anomaly profiles. Then standard linear interpolation techniques were used to integrate along the shelf break between moorings given their geographic location. Estimated alongshore spatial decorrelation scales of approximately 35 km were reported by Li et al. (1996) on the outer Louisiana-Texas continental shelf. The mean separation distance of the LATEX-A shelf break moorings is 67.7 km, generally exceeding these spatial decorrelation scales (Figure 1). Thus, we feel use of the present simple, conventional procedure for estimation of geostrophic transport is marginally justified along the Louisiana-Texas shelf break. While it will provide estimates of the cross-shelf geostrophic transport, it may miss some of the details of the spatial structure of this transport.

III. RESULTS

3.1 Modal Amplitudes Along the Louisiana-Texas Shelf Break

A comparison of first and second baroclinic mode amplitudes obtained from mooring data with those obtained in a pilot study from LATEX-A hydrographic data is shown in Figure 5. The hydrographic data was continuous in vertical resolution and sampled at every half meter in the water column, whereas mooring data is more limited in vertical resolution, but the modal amplitudes appear to be comparable. A comparison of the barotropic mode amplitudes is not illustrated in Figure 5 because the modal analysis was computed relative to different mean density in these two studies. The present reference density is a shelf break mean, instead of a shelf-wide mean, and this affects the magnitude of barotropic local vertical mode amplitudes at the shelf break. Hydrographic cruise data yields a “snapshot” of the temperature and salinity profiles at the time of the CTD cast. Although measurements are taken at no more than three depths in the water column, the time series available from LATEX-A moorings present sufficient degrees of freedom for a three mode analysis to provide some insight into the temporal variability of geostrophic transport across the shelf break.

Goodness of fit was addressed by comparing the adjusted pressure profiles computed from the modes and modal amplitudes using (9), to the observations at three levels in the water column at

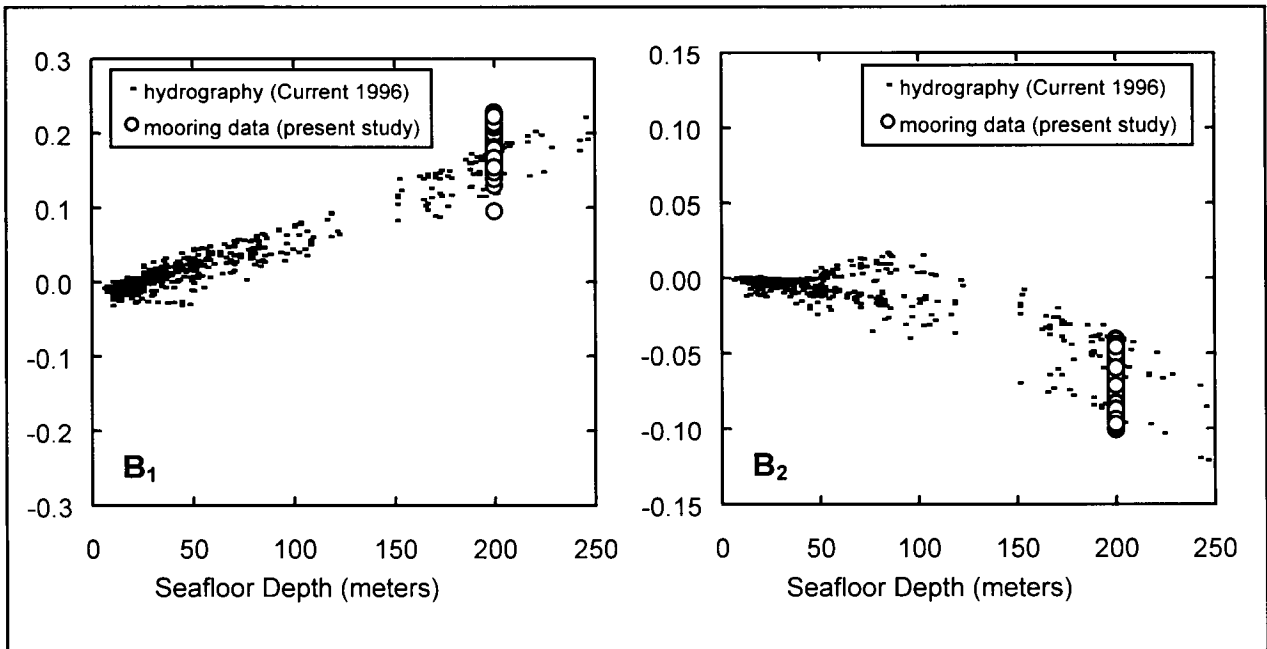


Figure 5. First and second baroclinic pressure anomaly mode amplitude coefficients B_n versus seafloor depth on the Louisiana-Texas shelf from LATEX-A cruise hydrography and from shelf break mooring data.

the same mooring and time. The modal fit accounted for 97% of the variance in the data from all 10 moorings during the time periods considered in this study. The fit was better in winter than in summer, and better at upcoast regions than downcoast. The residual includes contributions of higher modes, which were not addressed in this study, to the variance in the data.

An advantage of the present method of analysis is that the dynamic structure functions are based on linear dynamics that depend on the long wave assumption. Therefore they filter the data, removing high frequency and nonlinearities in the data that may otherwise obscure fundamental seasonal patterns. Loop Current eddies that persist in the outer shelf region are known to introduce nonlinearities to the circulation dynamics at the shelf break, and the present methodology is one way to remove these effects from a low frequency analysis. Statistics of modal amplitudes for pressure anomaly during summer, fall, winter, and spring indicate that the absolute value of the first baroclinic mode amplitude tends to be higher during the winter than during the summer. The reverse is true for the second baroclinic mode amplitude. In fact, for both baroclinic modes the ranges in amplitudes for winter and for summer seasons do not intersect, i.e. the observed differences are statistically significant. Seasonal statistics of B_0 , B_1 , and B_2 modal amplitudes are given in Table 1 including the percent each mode contributes to the total variance accounted for by all three modes. The seasonal pattern of mean modal amplitudes is illustrated in Figure 6. Throughout the present study, spring is taken to be March, April and May, summer is June, July, and August, fall is September, October, and November, and winter is December, January, and February.

Clearly the summertime is characterized by greater contribution of the higher (second) baroclinic mode to the modal representation of the pressure anomaly profile. In the summertime, second baroclinic mode mean and median amplitudes are larger in absolute value than during other seasons. Second baroclinic mode amplitudes were greater in absolute value than 0.09 only during the summer month of June, and the highest second baroclinic mode amplitude occurred June 27 at mooring 5, the southernmost mooring analyzed for that time period. No July, August, or September analyses were conducted. The second baroclinic and higher modes appear to be required to adequately represent the effects of near surface summer heating. First baroclinic mode amplitudes are lowest in summer, and barotropic mode amplitudes are low as well (Table 1).

In the late winter and early spring first baroclinic mode amplitudes were high, and these were distinctly higher at upcoast moorings than at those moorings further downcoast (Figure 6). Second baroclinic mode amplitudes were low in absolute values shelf-wide during late winter, with a small range and standard deviation. The smaller second baroclinic mode amplitudes of winter may reflect the absence of strong heating at the sea surface and deepening of the mixed layer. Mean and median barotropic mode amplitudes are large in the winter but greatest in the springtime and smallest in the fall.

The spatial distribution of vertical dynamic modes of pressure anomaly along the shelf break was examined by compiling basic statistics (Table 2) for the downcoast region (moorings 4, 5, and 6), the midshelf region (moorings 7, 8, 9, and 10) and the upcoast region (moorings 11, 48, and 13). The locations of these moorings can be seen in Figure 1. Despite considerable differences

Table 1. Seasonal statistics of barotropic, first baroclinic, and second baroclinic mode amplitudes for 144 15-day mean pressure profiles on the Louisiana-Texas shelf break. Seasons are summer (June), fall (October, November), winter (February), and spring (March, April, May). The notation $\langle B_n^2 \rangle$ indicates the mean square mode n amplitude coefficient.

Mode	Statistic	Summer	Fall	Winter	Spring	All
Barotropic	Mean	0.69	0.67	0.71	0.72	0.71
	Median	0.70	0.67	0.71	0.72	0.71
	Std Dev	0.02	0.01	0.01	0.01	0.03
	Maximum	0.72	0.70	0.74	0.75	0.75
	Minimum	0.60	0.64	0.69	0.69	0.60
	$\langle B_0^2 \rangle$	0.48	0.45	0.51	0.52	0.50
	% variance	91.1	90.8	89.5	89.7	90.0
First Baroclinic	Mean	0.15	0.16	0.20	0.19	0.18
	Median	0.15	0.16	0.20	0.20	0.18
	Std Dev	0.02	0.01	0.01	0.02	0.03
	Maximum	0.18	0.18	0.23	0.23	0.23
	Minimum	0.09	0.14	0.18	0.16	0.09
	$\langle B_1^2 \rangle$	0.02	0.03	0.04	0.04	0.03
	% variance	4.4	5.5	7.2	6.6	6.1
Second Baroclinic	Mean	-0.09	-0.06	-0.04	-0.06	-0.06
	Median	-0.09	-0.06	-0.04	-0.06	-0.06
	Std Dev	0.01	0.01	0.00	0.01	0.02
	Maximum	-0.07	-0.04	-0.04	-0.04	-0.04
	Minimum	-0.10	-0.09	-0.05	-0.09	-0.10
	$\langle B_2^2 \rangle$	0.01	0.00	0.00	0.00	0.00
	% variance	1.6	0.7	0.4	0.7	0.8

in shelf topography and geometry, the differences in dynamic modal amplitudes between regions were not remarkable without separation of seasons. Most notable was the slightly greater contribution of the first baroclinic mode to the variance accounted for by the first three modes in the upcoast region compared with the midshelf or downcoast regions. This difference occurred during February through April (Figure 6) at moorings 11, 13, and 48. However the differences in response due to location along the Louisiana-Texas shelf break are minor in comparison with the observed seasonal cycles of modal amplitude.

3.2 Dynamic Height

Although coastal sea level depends on the combination of factors including thermally-induced, wind-induced, and riverine-induced annual signals, mean sea level at the shelf break in the Gulf of Mexico is strongly influenced by the annual steric signal. Pattullo et al. (1955) describe seasonal oscillations in sea level. Whitaker (1971) describes the annual shelf break steric signal in the Gulf of Mexico and Sturges and Blaha (1976) interpret these findings. Whitaker showed

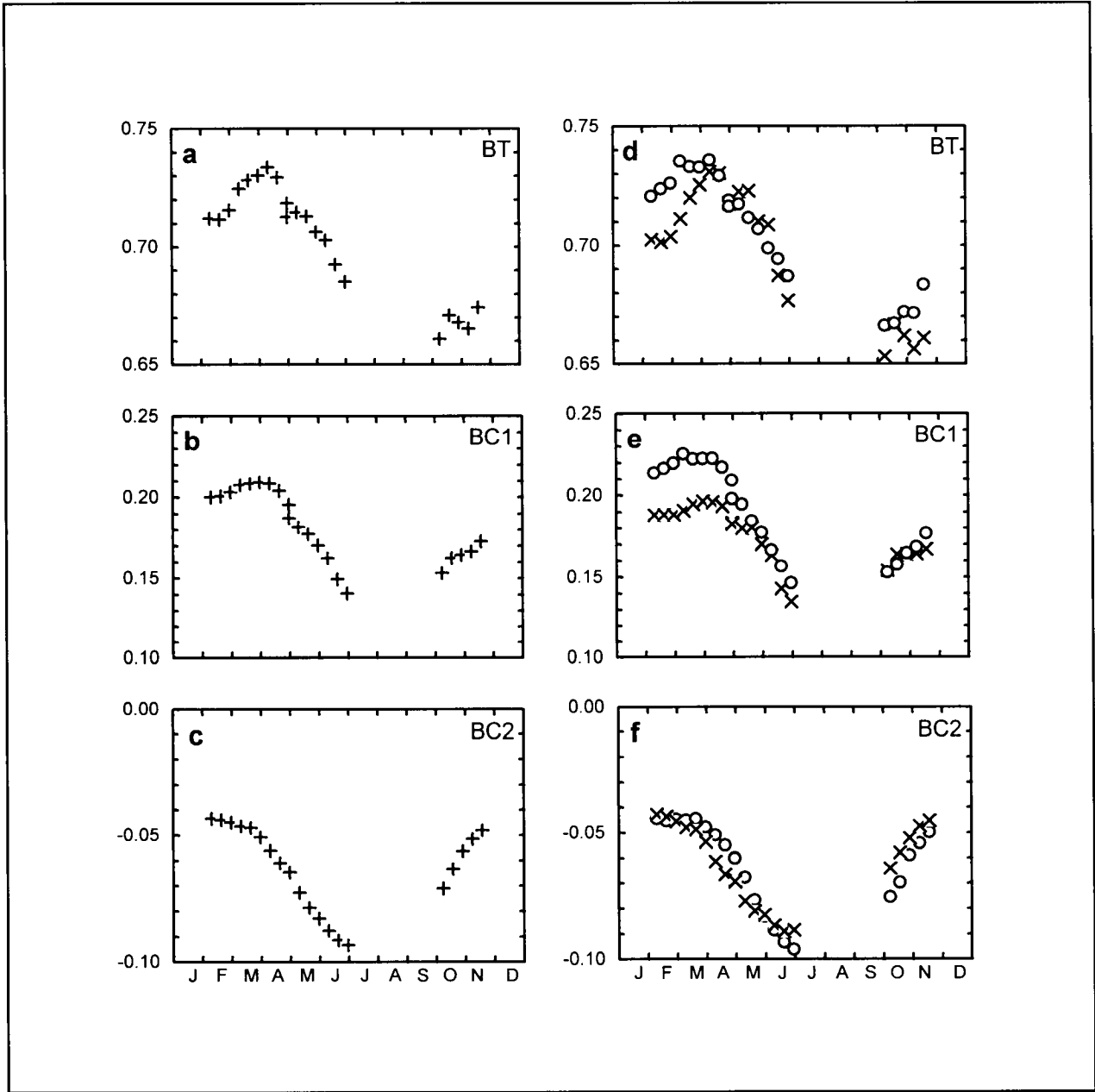


Figure 6. Monthly shelf-wide modal amplitude means for (a) barotropic, (b) first baroclinic, and (c) second baroclinic modes. Upstream (o) and downstream (x) modal amplitude means for (d) barotropic, (e) first baroclinic, and (f) second baroclinic modes. Here the upstream region encompasses moorings 11, 48, and 13, and the downstream region refers to moorings 4, 5, and 6.

Table 2. Alongshore regional statistics of modal amplitudes for the 144 15-day mean pressure profiles on the Louisiana-Texas shelf break. Downcoast region is moorings 4, 5, and 6. Midshelf region is moorings 7, 8, 9, and 10. Upcoast region is moorings 11, 48, and 13. The notation $\langle B_n^2 \rangle$ indicates the mean square mode n amplitude coefficient.

Mode	Statistic	Downcoast	Midshelf	Upcoast	Total
Barotropic	Mean	0.70	0.71	0.71	0.71
	Median	0.70	0.71	0.72	0.71
	Std Dev	0.03	0.02	0.02	0.03
	Maximum	0.74	0.74	0.75	0.75
	Minimum	0.60	0.67	0.66	0.60
	$\langle B_0^2 \rangle$	0.49	0.50	0.51	0.50
	% variance	90.4	90.5	89.3	90.1
First Baroclinic	Mean	0.18	0.18	0.20	0.18
	Median	0.18	0.17	0.21	0.18
	Std Dev	0.02	0.02	0.03	0.03
	Maximum	0.20	0.21	0.23	0.23
	Minimum	0.09	0.14	0.14	0.09
	$\langle B_1^2 \rangle$	0.03	0.03	0.04	0.03
	% variance	5.7	5.6	6.9	6.1
Second Baroclinic	Mean	-0.06	-0.07	-0.06	-0.06
	Median	-0.06	-0.07	-0.06	-0.06
	Std Dev	0.02	0.02	0.02	0.02
	Maximum	-0.04	-0.04	-0.04	-0.04
	Minimum	-0.10	-0.10	-0.10	-0.10
	$\langle B_2^2 \rangle$	0.00	0.00	0.00	0.00
	% variance	0.8	0.9	0.7	0.8

that there is a very large thermally induced range (order 13 cm) in water level off the Texas shelf break. In fact, Whitaker found an essentially common annual signal of steric water level throughout the northern and western part of the Gulf of Mexico, in particular near the shelf break off Cedar Keys, Pensacola, Eugene Island, Galveston, and Tampico. This signal was characterized by a single minimum close to the time of the vernal equinox, and a single maximum near the autumnal equinox.

The annual steric water level signal for the Louisiana-Texas shelf break was approximated using estimates of the mean steric water level for winter, spring, summer and fall near the shelf break at 94°W that were obtained from the data provided by a combination of 12 LATEX A and C surveys from 1992 – 1994. A Fourier fit using the annual and semiannual periods gives a representation of the annual steric signal very similar to that of Whitaker (1971) but with a slightly smaller range. Figure 7 depicts these seasonal means from the hydrographic cruises and the Fourier fit to them as presented in Current (1996). Estimates of the mean steric water level across the Louisiana-Texas shelf 200-m isobath for all four seasons were obtained from the 10 shelf break moorings of Figure 1, and these estimates were adjusted by an annual mean

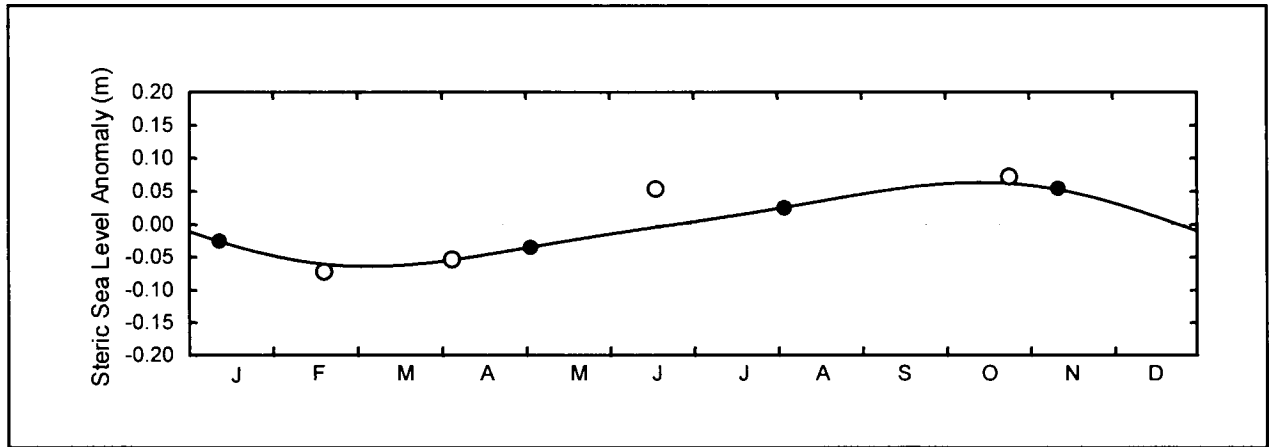


Figure 7. Two component Fourier fit to seasonal steric water level averages computed from LATEX hydrographic cruise data (filled circles) at about 94°W near the 200-m isobath on the Louisiana-Texas continental shelf. Open circles represent seasonal steric water level averages computed from LATEX-A shelf break mooring data. The annual mean has been removed.

representing equal weighting of the four seasonal means. These seasonal values from the 10 shelf break moorings are also shown in Figure 7.

The seasonal mean steric water level from the shelf break moorings agrees well with the fitted curve computed from the LATEX-A hydrographic data, with the exception of summer water level, which is high. This is consistent with the much poorer modal fit of the data in June 1992 than during other months. Seasonal surface heating and runoff results in more energy being moved into the higher modes for adequate modal representation of the data, but due to the degrees of freedom available the study was limited to three dynamic modes. The energy corresponding to baroclinic modes three and higher is responsible for a higher residual, and some aliasing of this energy into lower modes may have occurred as well. Therefore the present methodology appears to be better suited to the non-summer months or to hydrographic data with its many levels of measurement.

3.3 Transport Across the Louisiana-Texas Shelf Break

Estimated 15-day mean transports for specific depth ranges in the water column are listed by alongshore region in Table 3, and for the entire shelf in Table 4. The depth ranges evaluated are 0-70 meters and 70-200 meters, as well as for the entire 200 meter water column.

Although geostrophic transport across the Louisiana-Texas shelf break was offshore in the upper 70 meters of the water column during the spring of 1992, onshore flow was substantial in deeper waters during this time particularly in the upcoast region. By late June, transport was essentially onshore in direction throughout the water column. In October 1992, the direction of transport

Table 3. Estimated transport (in Sverdrups) off the Louisiana-Texas shelf at the 200-meter isobath, listed by alongshelf region at specified depth ranges. The downcoast region extends from LATEX-A mooring 4 to mooring 7 and includes the south Texas shelf. The midshelf region extends from mooring 7 to mooring 10, and the upcoast region includes the shelf break from mooring 10 to mooring 13 (see Figure 1 for mooring locations). Offshore flow is positive.

	0-70 meters			70-200 meters		
	Downcoast	Midshelf	Upcoast	Downcoast	Midshelf	Upcoast
April 28, 1992	0.32	0.24	-0.10	0.19	-0.16	-0.41
May 8, 1992	0.09	0.27	0.02	0.12	-0.22	-0.29
May 18, 1992	0.18	-0.08	0.13	0.30	-0.30	-0.27
May 28, 1992	0.35	-0.06	0.17	0.51	-0.25	-0.30
June 7, 1992	0.24	-0.14	0.26	0.31	-0.28	-0.25
June 17, 1992	0.10	-0.17	0.25	0.17	-0.28	-0.17
June 27, 1992	-0.17	-0.40	0.18	0.04	-0.37	-0.16
October 3, 1992	-0.26	0.39	-0.30	-0.22	0.36	0.19
October 13, 1992	-0.08	0.24	-0.31	-0.18	0.23	0.24
October 23, 1992	-0.18	0.39	-0.34	-0.31	0.32	0.22
November 2, 1992	-0.09	0.34	-0.13	-0.32	0.33	0.39
November 12, 1992	0.05	0.34	0.03	-0.20	0.26	0.52
February 7, 1993	0.22	0.22	0.34	0.13	-0.12	0.21
February 17, 1993	0.49	0.12	0.43	0.27	-0.16	0.28
February 27, 1993	0.01	0.42	0.36	-0.01	-0.01	0.19
March 9, 1993	0.46	0.35	0.19	0.26	-0.10	0.16
March 19, 1993	0.17	0.29	0.10	0.18	-0.14	0.09
March 29, 1993	-0.19	0.55	-0.04	-0.11	0.04	-0.06
April 8, 1993	-0.27	0.64	-0.23	-0.25	0.09	-0.21
April 18, 1993	-0.21	0.54	-0.32	-0.27	0.07	-0.32
April 28, 1993	-0.77	0.90	-0.29	-0.62	0.34	-0.40

Table 4. Estimated transport (in Sverdrups) off the Louisiana-Texas shelf at the 200-meter isobath, listed by alongshelf region for the full water column and also listed for the entire shelf break at specified depth ranges. The downcoast region extends from LATEX-A mooring 4 to mooring 7 and includes the south Texas shelf. The midshelf region extends from mooring 7 to mooring 10, and the upcoast region includes the shelf break from mooring 10 to mooring 13 (see Figure 1). Offshore flow is positive.

	0-200 meters			Shelf-wide		
	Downcoast	Midshelf	Upcoast	0-70 meters	70-200 m	0-200 m
April 28, 1992	0.51	0.08	-0.51	0.46	-0.37	0.08
May 8, 1992	0.21	0.05	-0.26	0.39	-0.38	0.00
May 18, 1992	0.48	-0.38	-0.14	0.23	-0.26	-0.04
May 28, 1992	0.86	-0.31	-0.14	0.46	-0.05	0.41
June 7, 1992	0.55	-0.41	0.01	0.36	-0.22	0.15
June 17, 1992	0.27	-0.45	0.08	0.17	-0.27	-0.10
June 27, 1992	-0.13	-0.77	0.02	-0.39	-0.49	-0.88
October 3, 1992	-0.48	0.74	-0.11	-0.17	0.32	0.15
October 13, 1992	-0.26	0.47	-0.07	-0.15	0.29	0.14
October 23, 1992	-0.49	0.71	-0.12	-0.13	0.24	0.10
November 2, 1992	-0.40	0.67	0.26	0.13	0.40	0.53
November 12, 1992	-0.14	0.59	0.55	0.42	0.58	1.00
February 7, 1993	0.35	0.10	0.55	0.77	0.23	1.00
February 17, 1993	0.76	-0.03	0.70	1.04	0.39	1.43
February 27, 1993	0.00	0.41	0.55	0.80	0.16	0.96
March 9, 1993	0.72	0.25	0.35	1.00	0.32	1.32
March 19, 1993	0.35	0.16	0.19	0.56	0.14	0.70
March 29, 1993	-0.30	0.59	-0.10	0.32	-0.13	0.19
April 8, 1993	-0.52	0.72	-0.44	0.14	-0.37	-0.23
April 18, 1993	-0.48	0.61	-0.64	0.01	-0.52	-0.51
April 28, 1993	-1.38	1.24	-0.69	-0.16	-0.68	-0.83

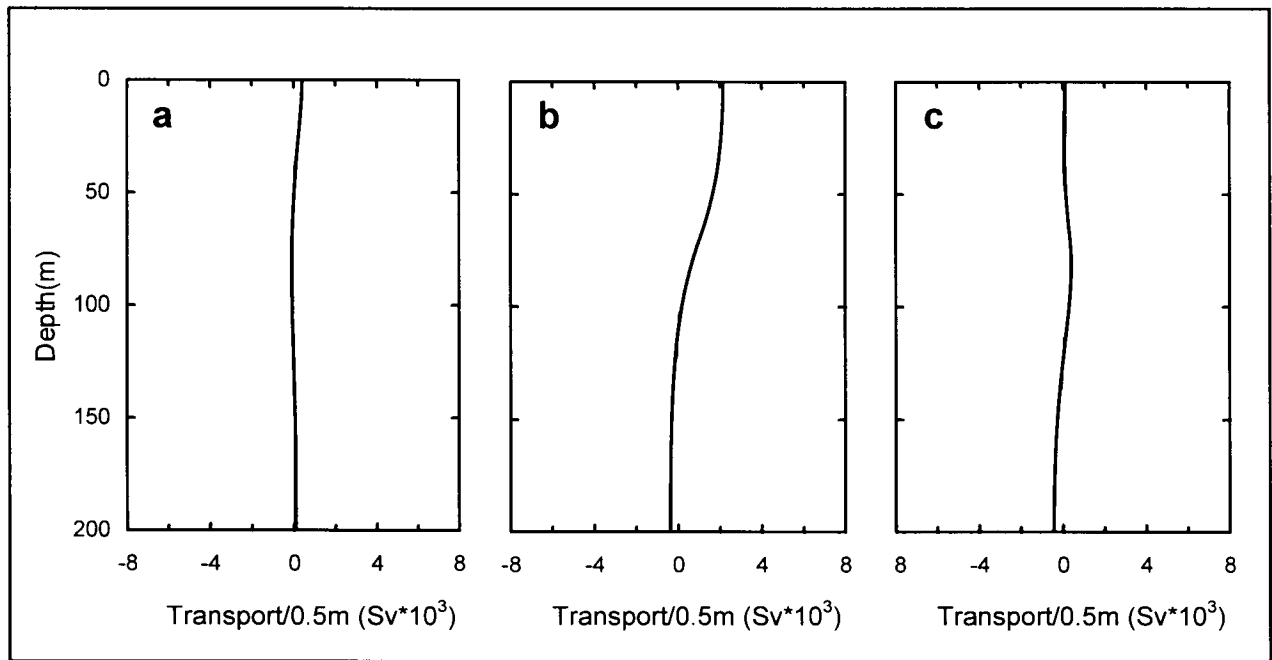


Figure 8. Mean offshore geostrophic transport per half meter depth across the Louisiana-Texas shelf break for (a) downcoast, (b) midshelf, and (c) upcoast Louisiana-Texas shelf break regions for time intervals treated in this study. Regions are defined as downcoast (mooring 4 to mooring 7), midshelf (mooring 7 to mooring 10), and upcoast (mooring 10 to mooring 13). Flow in the offshore direction is positive.

across the 200-m isobath was onshore in the upper 70 meters except in the midshelf region, and offshore in deeper waters except in the downcoast region. By November transport was offshore throughout the water column and remained so through February to mid-March. Onshore flow first appeared in deeper waters from 70-200 meters in late March and April 1993, and flow was onshore throughout the water column by the end of April 1993.

Flow across the shelf break is not unidirectional in the mean (Figures 8 and 9) or at any given time of year, but varies by depth and by location along the shelf break (Appendices A and B).

Seasonal average geostrophic transport profiles in the offshore direction across the Louisiana-Texas shelf are provided in Figure 9. In summer there is onshore mean transport in the deeper layers and offshore transport in the upper water column. In the fall, this offshore transport has deepened with a maximum around 82 meters decreasing to nearly zero at the bottom. Above 33 meters mean fall cross-isobath transport is onshore. Winter mean transport is strongly offshore in near surface waters from zero to 70 meters. Substantial offshore mean transport does not penetrate as deeply in the water column in spring as in winter.

Flow onto or off of the shelf in any given region may compensate for flow in the opposing direction elsewhere across the shelf break or for alongshelf flow. Often the direction of flow

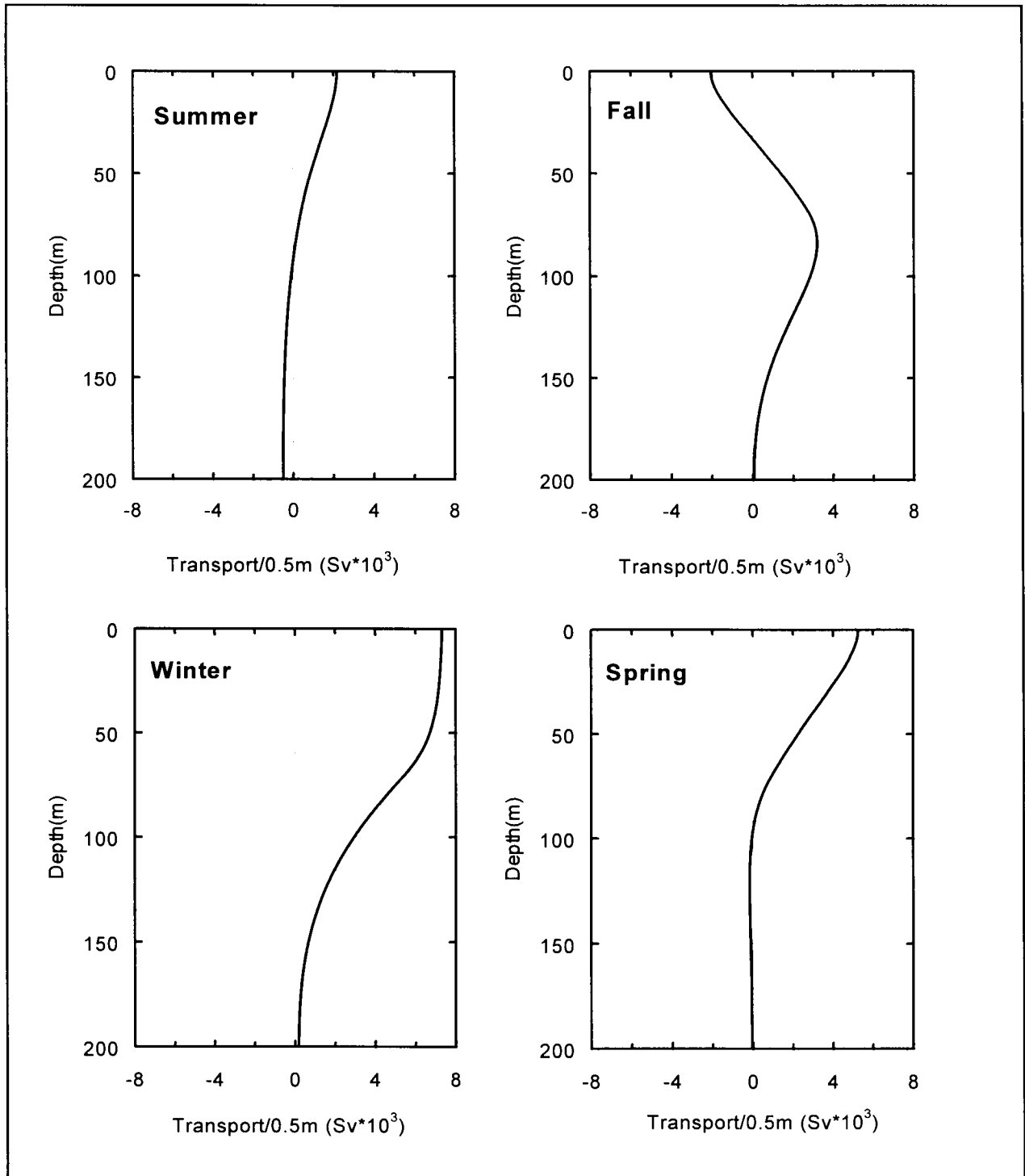


Figure 9. Seasonal average geostrophic transport per half meter depth in the offshore direction across the Louisiana-Texas shelf break. Seasons are defined as summer (June, July, August), fall (September, October, November), winter (December, January, February), and spring (March, April, May). Offshore direction is positive.

across the 200-m isobath appears to differ in the midshelf region from the direction in the upcoast and downcoast regions, and this is more frequently the case in the upper 70 meters of the water column. Flow in this upper layer was offshore in the midshelf region but onshore elsewhere from the beginning of October through mid-November 1992, and from the end of March through April 1993. This was also true in the lower layer during the latter time period. Upper layer onshore flow occurred only in the midshelf region from mid-May through June 1992. The data coverage was insufficient to allow a complete mass balance for the shelf.

Mean profiles of geostrophic transport in the offshore direction at the 200-m isobath were obtained for upcoast, midshelf, and downcoast regions of the Louisiana-Texas shelf break and are depicted in Figure 8. Comparing Figure 8 and Figure 9 it is apparent that cross-shelf transport differs by season more than it differs by alongshelf location. Upper layer offshore geostrophic transport in the midshelf region was robust during October and April of 1992, when the direction of transport was towards the coast in other regions of the shelf. This may explain the overall offshore transport in the upper layer over the midshelf region. Offshore transport as a function of position on the 200-m isobath at 10 day intervals can be found in Appendix B, Figures B1 through B4, and as time series by region in Figure B5. The strongly offshore transport between moorings 9 and 10 in late April 1992 appears to move gradually downshelf and by early June occurs between moorings 8 and 9 (Figure B1). Transport on June 17 and June 27, 1992, was very large in the onshore direction at mooring 5 and in the offshore direction at mooring 6. Summer heating may have allowed considerable energy to move into the higher baroclinic modes, resulting in aliasing of this energy and the consequently poorer fit obtained during the summer in the downcoast region when using only three modes. This may be partially responsible for the large transports in the downcoast region during June 1992. It appears that the strongly offshore geostrophic transport observed in April and May between moorings 5 and 6 moved further north between moorings 6 and 7 in mid-June and later June and this is accompanied by a reversal and very strongly onshore geostrophic transport between moorings 5 and 6. These changes are apparently associated with the alongshelf current reversal on the inner shelf that occurred during mid-June of 1992 (Nowlin et al. 1998).

Vertical profiles of shelf-wide geostrophic mean transport at ten day intervals are provided in Appendix A. These sequences of high resolution profiles of offshore transport reveal smooth and gradual transitions between seasons.

IV. DISCUSSION

The cyclonic circulation pattern suggested by Cochrane and Kelly (1986) for the Louisiana-Texas shelf includes offshore flow at the southwestern (downcoast) part of the shelf break and onshore transport in the northeastern (upcoast) part, to complete the gyre, during non-summer months. During summer, the Cochrane and Kelly rendition of shelf-wide circulation specifies the break down and reversal of non-summer patterns.

The LATEX program, funded by the MMS in the early 1990's, presented a new wealth of knowledge and detail pertaining to circulation patterns on the Louisiana-Texas continental shelf. Comparison of results obtained by the LATEX-A scientists with Cochrane and Kelly's earlier concept of overall circulation patterns on the Louisiana Texas shelf were equivocal, especially with respect to the outer shelf (Nowlin et al. 1998). Inner shelf currents were observed to flow in the downcoast direction during non-summer months, reversing to flow upcoast in the summer as outlined by Cochrane and Kelly. Monthly averaged currents along the outer shelf edge were not often in the same alongshore direction, although mean alongshore currents over the 32 months of LATEX-A data were upcoast over the outer shelf. However no coherent pattern to the annual signal on the outer shelf was determined in the LATEX analyses, and while cross-shelf currents at the shelf break must ultimately maintain continuity it is thought that they may be primarily due to offshore eddies. The large interannual variability on the outer shelf is attributed to anticyclonic rings such as Eddy Vazquez, which is thought to be responsible for the strong upcoast flow observed by the LATEX program in south Texas in 1993 (Nowlin et al. 1998). In a study based on LATEX-A data as well as *M/V Gus III* cruises and other historical data, high surface salinities exceeding 36.0 that extend through the water column were observed to move upcoast as far as central Texas in the summer (Li et al. 1997). In other seasons, water on the Texas shelf is fresher and this is presumably due to downcoast flow transporting fresh water outflow from the Mississippi and Atchafalaya River systems onto the Texas shelf. The annual cycle of freshwater volume on the Louisiana-Texas shelf is known to be dominated by the spring flood of the Mississippi/Atchafalaya rivers (Dinnel and Wiseman 1986).

The results presented in this report provide an additional analysis of cross-shelf geostrophic transport at the shelf break during parts of 1992 and 1993, that is *not* generally consistent with Cochrane and Kelly's analysis of summer and non-summer mean cross-shelf transport. Mean seasonal cross-shelf geostrophic transports are listed in Table 5. Although Cochrane and Kelly's summer was July-August, months that were not analyzed in the present study, June 1992 patterns of cross-shelf transport at the shelf break were used to estimate the summer mean transport. The downcoast region as defined here extends from mooring 4 to mooring 7, the midshelf region extends from mooring 7 to mooring 10, and the upcoast region extends from mooring 10 to mooring 13 (see Figure 1).

In the downcoast (southern) shelf break region, mean non-summer cross-shelf flow was onshore although net flow in this region was small, and mean summer cross-shelf flow was offshore. This is not consistent with the analysis of Cochrane and Kelly (1986) in which flow across the shelf break was away from the coast in the non-summer. Analysis of the midshelf region reveals

Table 5. Mean seasonal estimated offshore geostrophic transport at the Louisiana-Texas shelf break in Sverdrups ($10^6 \text{ m}^3/\text{s}$).

	Downcoast	Midshelf	Upcoast	All
Fall	-0.36	0.64	0.10	0.38
Winter	0.37	0.16	0.60	1.13
Spring	0.03	0.23	-0.18	0.08
Summer	0.23	-0.54	0.03	-0.28
Non-summer	-0.01	0.37	0.00	0.36
Mean	0.02	0.24	0.00	0.26

substantial mean non-summer offshore flow and summer onshore flow occurred. However the small mean summer offshore flow and near zero mean non-summer flow in the upcoast (eastern) regions is not consistent with Cochrane and Kelly's findings of flow towards the shore across the eastern shelf break during non-summer seasons.

The LATEX-A box model study by Bender and Reid (Nowlin et al. 1998) provides information on cross-shelf transport (both geostrophic and ageostrophic) at the shelf break, whereas the present study quantifies geostrophic transport only. There is good qualitative agreement and some quantitative agreement between the two studies, which is not unreasonable considering that Chen (1995) found that 70% of the variance in the LATEX-A ADCP data was geostrophic and 30% ageostrophic. The estimated correlation coefficient for monthly averaged shelf-wide transport across the 200-m isobath from the two studies is 0.72, corresponding to an r^2 of 0.52, and 100% of shelf-wide monthly average transports were of the same sign (onshore or offshore). Regional monthly averages from the two studies were not as well correlated. The estimated correlation of monthly averaged transports across the shelf break for downcoast, midshelf, and upcoast regions treated separately was 0.49 with a corresponding r^2 of 0.24.

Qualitative agreement between the Bender and Reid study and the present study was still good for these regional monthly averages, having the same direction of monthly averaged regional cross-shelf flow 76% of the time (Table 6). The two differences in cross-shelf direction of flow in the upcoast region were the two smallest in absolute value of mean flow in the present study. The differences in the downcoast region are not as small, but the discrepancies occurred during months when data from mooring 4 was incomplete and the transport between moorings 4 and 5 was not analyzed. The southernmost edge of the Louisiana-Texas shelf is often the site of strong, persistent offshore jets which could not be resolved in the transport estimates computed for the present study, and may be responsible for the discrepancies between these two studies in the October and November 1992 directions of transport. Flow directions between mooring 7 and mooring 10 in the midshelf region of the shelf break agreed 100% of the time.

Table 6. Monthly average direction of cross-shelf flow at the shelf break (200-meter isobath) for the present study and for the Bender study (in parentheses). Direction of flow coincided 76% of the time. Mean offshore flow is denoted (+), mean onshore flow is denoted (-).

	This study (Bender study)		
	Downcoast	Midshelf	Upcoast
May '92	+ (+)	- (-)	- (-)
Jun '92	+ (-)	- (-)	+ (-)
Oct '92	- (+)	+ (+)	- (+)
Nov '92	- (+)	+ (+)	+ (+)
Feb '93	+ (+)	+ (+)	+ (+)
Mar '93	+ (+)	+ (+)	+ (+)
Apr '93	- (-)	+ (+)	- (-)

The geostrophic transports reported in this study appear large, but are consistent in range with those computed by the LATEX-A program. Offshore transport over the entire shelf was highest in the winter months, with average shelf-wide offshore transport of 0.76, 1.13, and 0.74 Sv for the months of November, February, and March respectively. Onshore transport was greatest in spring and summer, with average shelf-wide onshore transport of 0.28 Sv and 0.52 Sv during the months of June 1992 and April 1993. Oey (1995) found his modeled westward transport integrated from shore to the 30-m isobath to be comparable to that observed, about 0.15 Sv from the coast to the 30 meter isobath, though as high as 0.25 Sv in the fall. Bender and Reid report transport on the inner shelf is strongly downcoast averaging more than 0.25 Sv, and considerably greater alongshore flow on the outer shelf than the inner shelf. Cross-shelf flux over the 200-m isobath is generally stronger than the outer shelf alongshore fluxes (Nowlin et al. 1998). The mean transport across the shelf break in the present study is 0.26 Sv (Table 5).

Bender and Reid saw no seasonality of outer shelf transport, either alongshore or cross-shelf. However the high resolution profiles of cross-shelf transport presented in Appendix A suggest a slow, smooth seasonal progression of vertical patterns of mean cross-shelf geostrophic flow.

V. SUMMARY AND CONCLUSIONS

This study applies dynamic modal analysis techniques to LATEX-A mooring data to estimate time dependent, highly vertically resolved geostrophic transport across the Louisiana-Texas continental shelf break as well as dynamic height at mooring locations. Mean steric water level anomaly from the shelf break moorings is consistent with the smooth annual cycle determined from cruise hydrography by Current (1996), and is notably similar to the findings of Whitaker (1971). Geostrophic transport profiles also vary smoothly with season. Offshore transport is strong in the upper 70 meters of the water column during the winter. During the summer, onshore transport develops first in deeper waters, penetrating higher in the water column until eventually the direction of transport is onshore from surface to seafloor.

The scope of this study is limited to cross-shelf geostrophic flow on the 200-m isobath, and the implications of the present findings for the overall pattern of circulation on this continental shelf are as yet unknown. Transport profiles are influenced less by alongshore location on the shelf than by the time of year. Results of this study are consistent with the findings of the Texas-Louisiana Shelf Circulation and Transport Processes Study (LATEX-A), but provide high resolution vertical profiles of geostrophic transport previously unavailable to MMS.

Dinnel and Wiseman (1986) describe the large freshwater discharge of the Mississippi-Atchafalaya river systems onto the shelf in the springtime, where it travels downcoast with the prevailing currents. During the summer, this excess freshwater migrates upcoast with the summer reversal of winds over the Louisiana-Texas shelf. However, by November Dinnel and Wiseman observed that freshwater volume on the shelf is low. The very strong offshore flow east of 95°W observed in this study during November is not inconsistent with these prior observations. This offshore direction of flow east of 95°W was confirmed by the Bender and Reid study (Nowlin et al., 1998).

The circulation scheme proposed for the Louisiana-Texas shelf by Cochrane and Kelly (1986) has been confirmed for alongshore circulation on the inner shelf by several studies including Nowlin et al. (1998). However, the cross-shelf transport patterns put forth by Cochrane and Kelly to attain mass balance for the shelf has not been substantiated by the present study or by the Bender and Reid study described in Nowlin et al. (1998). This continental shelf continues far beyond the Mexican border. Future investigators may find it productive to examine the possibility that variability in alongshelf flow northward from Mexican waters on the outer shelf may be a key to understanding mass balance on the Louisiana-Texas shelf.

LITERATURE CITED

- Arango, H. and R. O. Reid. 1990. A generalized reduced-gravity ocean model. *Atmos.-Ocean* 29:256-287.
- Chen, H. –W. 1995. Variability and structure of currents over the Texas-Louisiana shelf—a view from a shipboard acoustic Doppler current profiler. Ph.D. Dissertation. Texas A&M University, Dept. of Oceanography, College Station, TX. 117 pp.
- Cho, K., R. O. Reid, and W. D. Nowlin Jr. 1998. Objectively mapped streamfunction fields on the Texas-Louisiana shelf based on 32 months of moored current meter data. *J. Geophys. Res.* 103:10377-10390.
- Cochrane, J. D. and F. J. Kelly. 1986. Low-frequency circulation on the Texas-Louisiana continental shelf. *J. Geophys. Res.* 91:10645-10659.
- Csanady, G. T. 1979. The pressure field along the western margin of the North Atlantic. *J. Geophys. Res.* 84:4905-4915.
- Current, C. L. 1993. Empirical vertical structure of density anomaly in the Gulf of Mexico. M.S. Thesis. Texas A&M University, Dept. of Oceanography, College Station, TX. 143 pp.
- Current, C. L. 1996. Spectral model simulation of wind driven subinertial circulation on the inner Texas-Louisiana shelf. Ph.D. dissertation. Texas A&M University, Dept. of Oceanography, College Station, TX. 144 pp.
- Dinnel, S. P. and W. J. Wiseman. 1986. Fresh water on the Louisiana and Texas shelf. *Cont. Shelf Res.* 6:765-784.
- Flierl, G. 1978. Models of vertical structure and the calibration of two-layer models. *Dyn. Atmos. Oceans* 2:341-381.
- Fofonoff, N. P. 1985. Physical properties of seawater: a new salinity scale and equation of state for seawater. *J. Geophys. Res.* 90:3332-3342.
- Kundu, P. K., J. S. Allen, and R. L. Smith. 1975. Modal decomposition of the velocity field near the Oregon coast. *J. Phys. Oceanogr.* 5:683-704.
- Li, Y., W. D. Nowlin Jr., and R. O. Reid. 1996. Spatial-scale analysis of hydrographic data over the Texas-Louisiana continental shelf. *J. Geophys. Res.* 101:20595-20605.
- Li, Y., W. D. Nowlin Jr., and R. O. Reid. 1997. Mean hydrographic fields and their interannual variability over the Texas-Louisiana continental shelf in spring, summer, and fall. *J. Geophys. Res.* 102:1027-1049.

- Nowlin, W. D. Jr., A. E. Jochens, R. O. Reid, and S. F. DiMarco. 1998. Texas-Louisiana Shelf Circulation and Transport Processes Study: Synthesis Report, Volume I: Technical Report. OCS Study MMS 98-0035. U.S. Dept. of the Interior, Minerals Management Service, Gulf of Mexico OCS Region, New Orleans, LA. 502 pp.
- Oey, L. -Y. 1995. Eddy- and wind-forced shelf circulation. *J. Geophys. Res.* 100:8621-8637.
- Pattullo, J., W. Munk, R. Revelle, and E. Strong. 1955. The seasonal oscillations in sea level. *J. Mar. Res.* (14)1:88-155.
- Science Applications International Corporation (SAIC). 1989. Gulf of Mexico Physical Oceanography Program, Final Report: Year 5. Volume II: Technical Report. OCS Report MMS 89-0068. U.S. Dept. of the Interior, Minerals Management Service, Gulf of Mexico OCS Region, New Orleans, LA. 333 pp.
- Sturges, W. and J. P. Blaha. 1976. A western boundary current in the Gulf of Mexico. *Science* (192)367-369.
- Whitaker, R. E. 1971. Seasonal variations of steric and recorded sea level of the Gulf of Mexico. M. S. Thesis. Texas A&M University, Dept. of Oceanography, College Station, TX. 111 pp.

APPENDIX A

VERTICAL PROFILES OF SHELFWIDE TRANSPORT

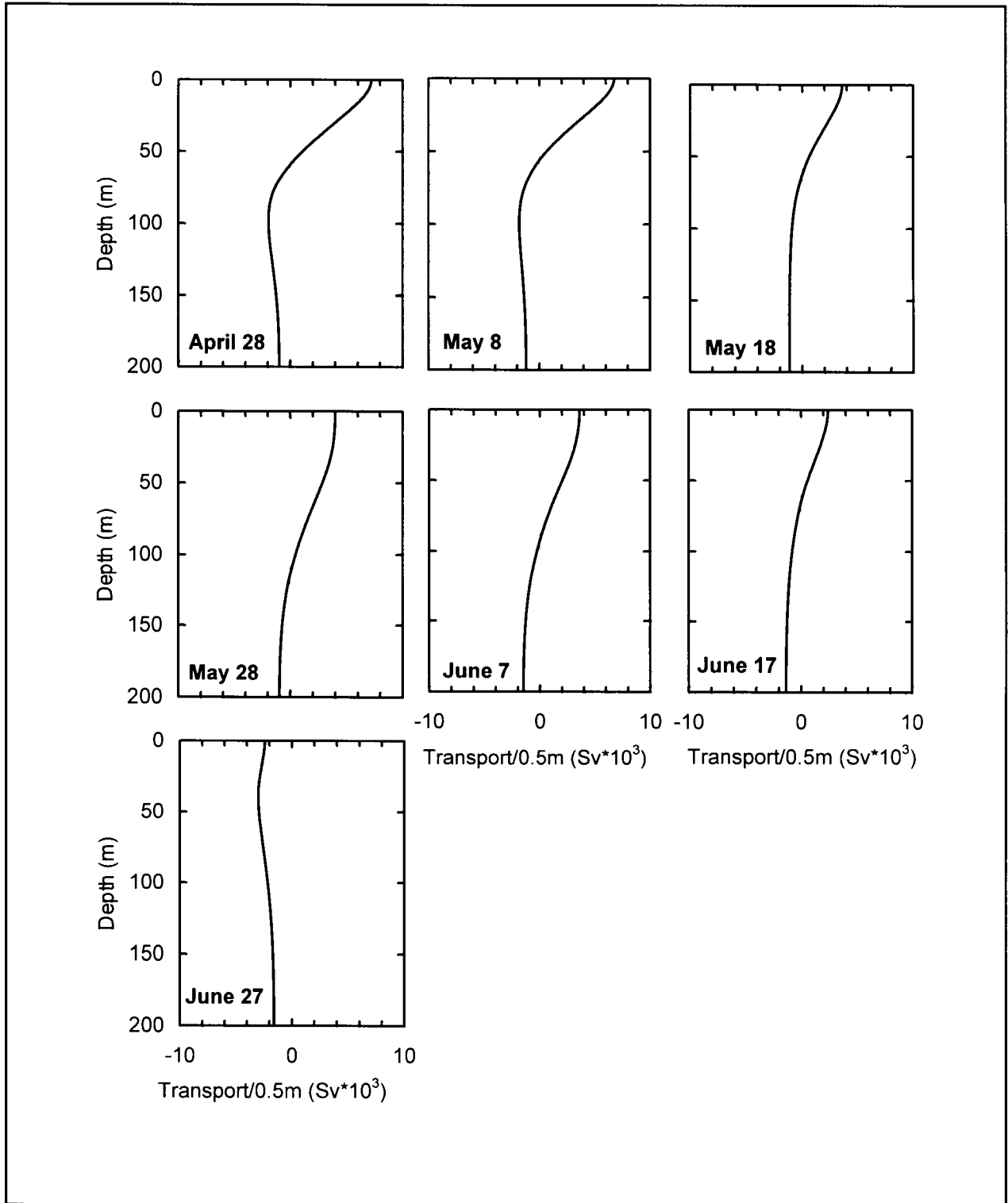


Fig. A1. Shelfwide transports per half meter depth in the offshore direction across the Louisiana-Texas shelf break, 15-day means from April 21 – July 3, 1992.

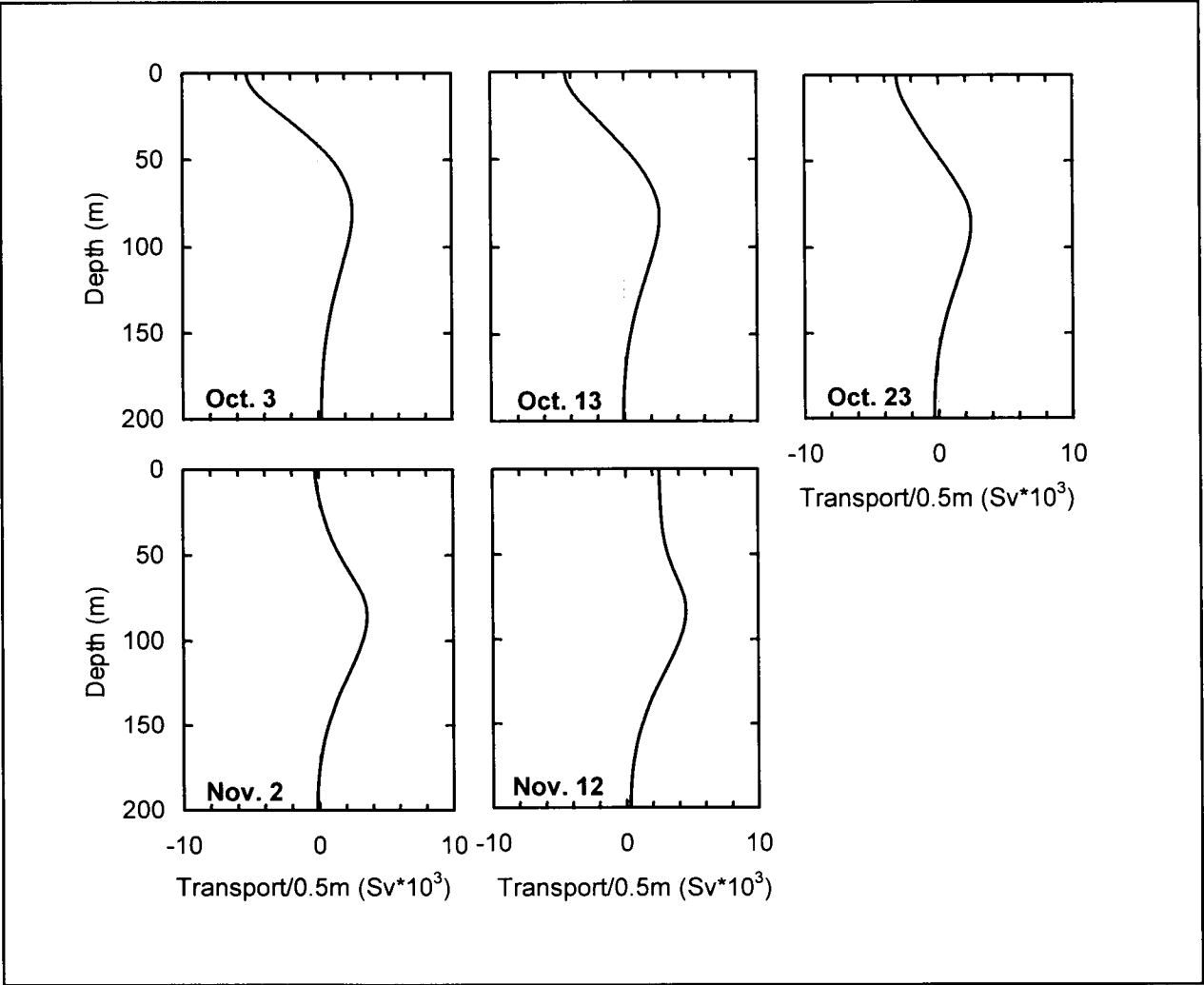


Fig. A2. Shelfwide transports per half meter depth in the offshore direction across the Louisiana-Texas shelf break, 15-day means from September 26 - November 19, 1992.

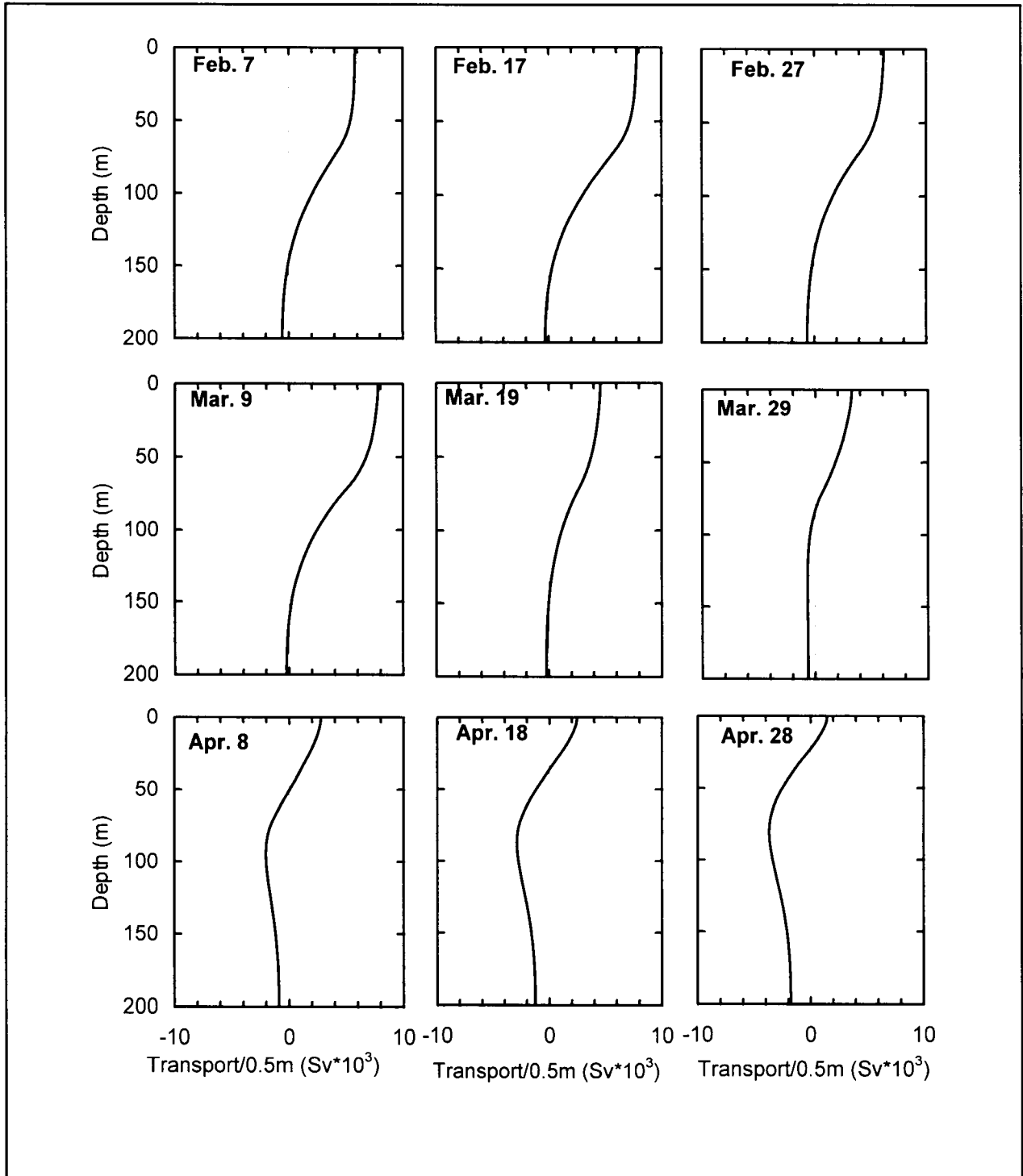


Fig. A3. Shelfwide transports per half meter depth in the offshore direction across the Louisiana-Texas shelf break, 15-day means from January 31 – May 5, 1993.

APPENDIX B

ESTIMATED TRANSPORT BY SHELF REGION

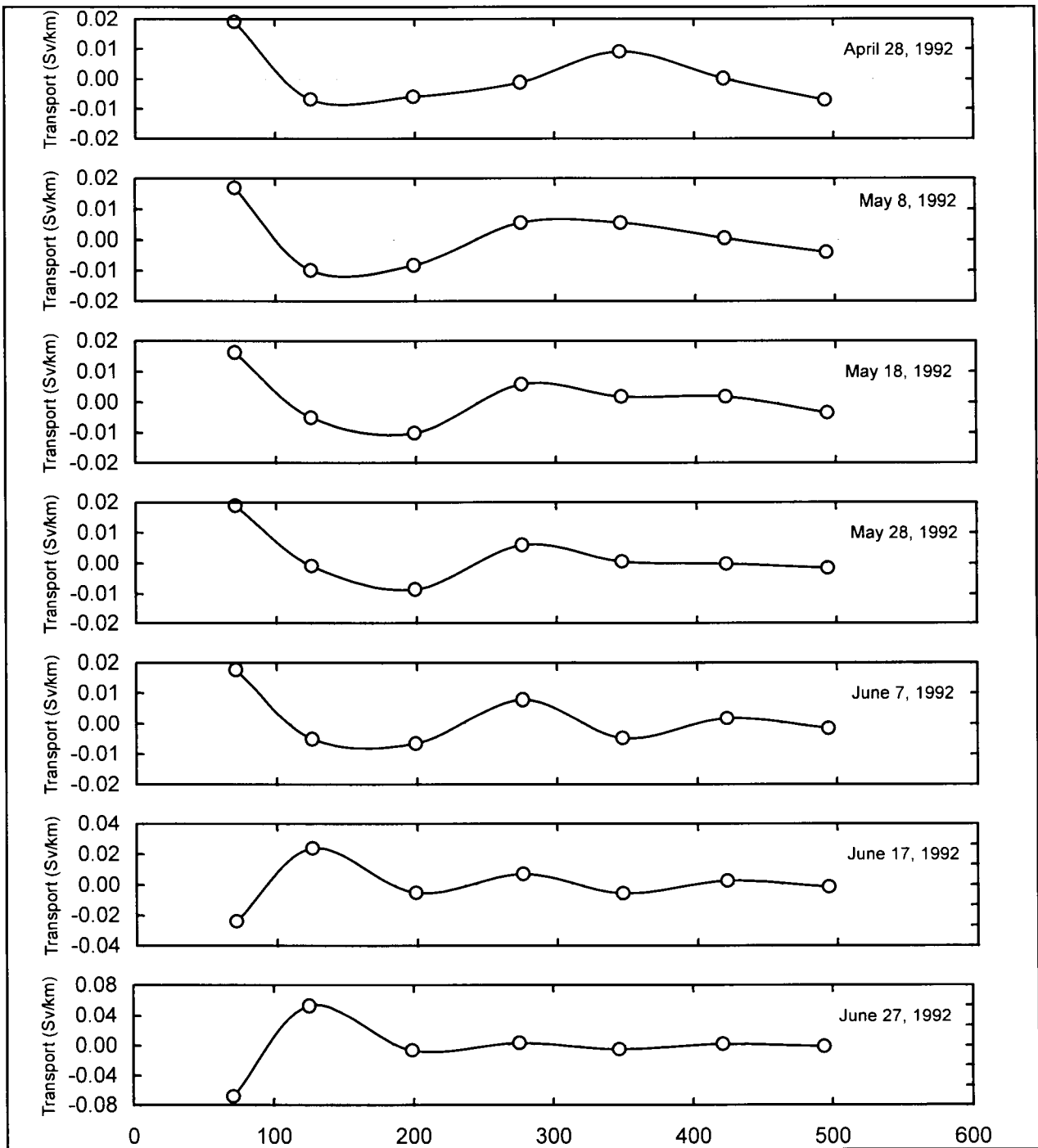


Figure B1. Estimated offshelf transport per km from April 28 – June 17, 1992, as a function of distance north and east along the 200-meter isobath from LATEX-A mooring 4. Circles represent locations half way between moorings 5, 6, 7, 8, 9, 10, 11, and 48. Notice the difference in transport scales on June 17th and 27th. Although the upshelf flow at this time was strong along the 200-meter isobath, it is thought that there may have been considerable energy in higher baroclinic modes during late June, causing an aliasing problem in accurate determination of transport.

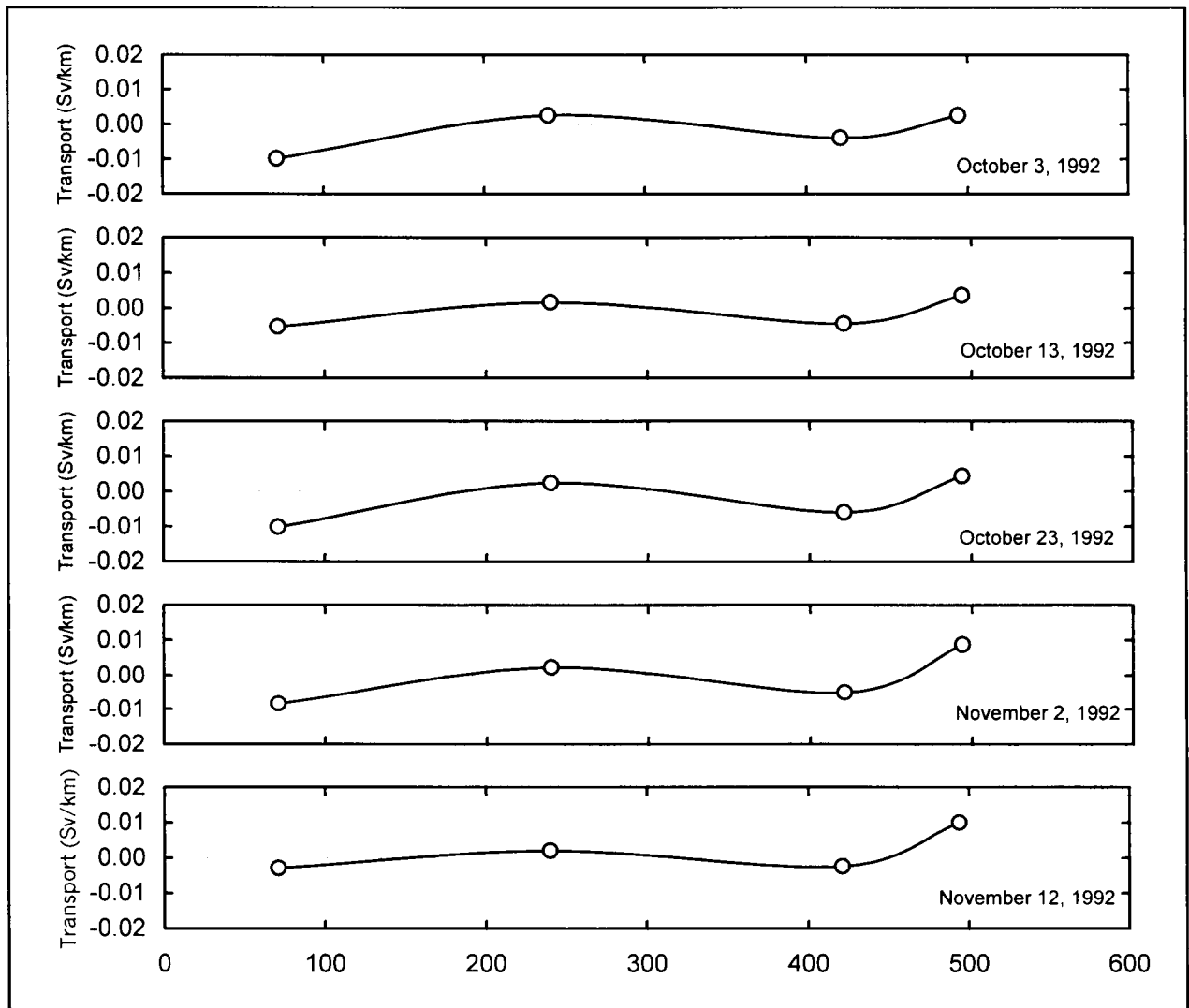


Figure B2. Estimated offshelf transport per km from October 3 – November 12, 1992, as a function of distance north and east along the 200-meter isobath from LATEX-A mooring 4. Circles represent locations half way between moorings 5, 6, 10, 11, and 48.

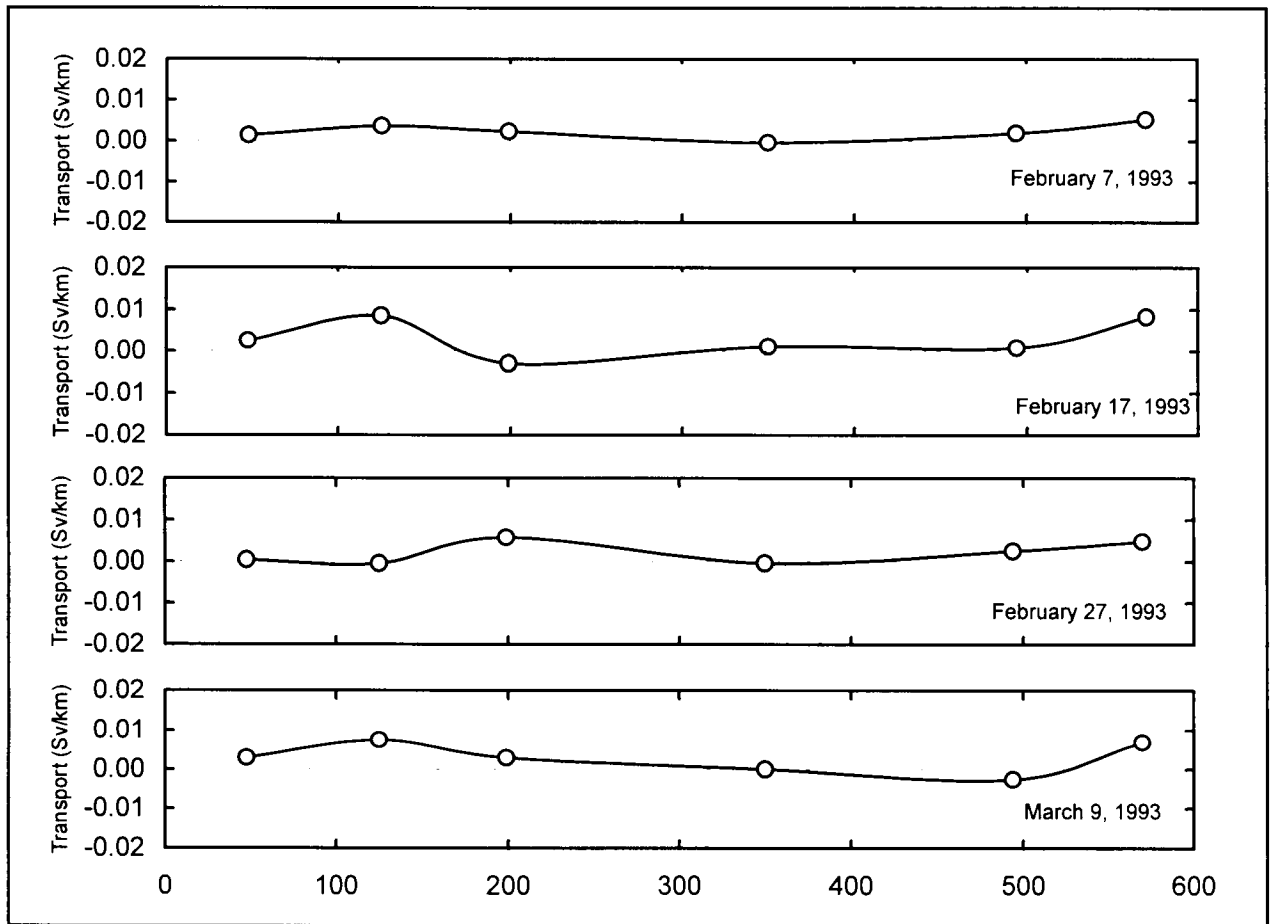


Figure B3. Estimated offshore transport per km from February 7 – March 9, 1993, as a function of distance north and east along the 200-meter isobath from LATEX-A mooring 4. Circles represent locations half way between moorings 4, 6, 7, 8, 11, 13, and 48.

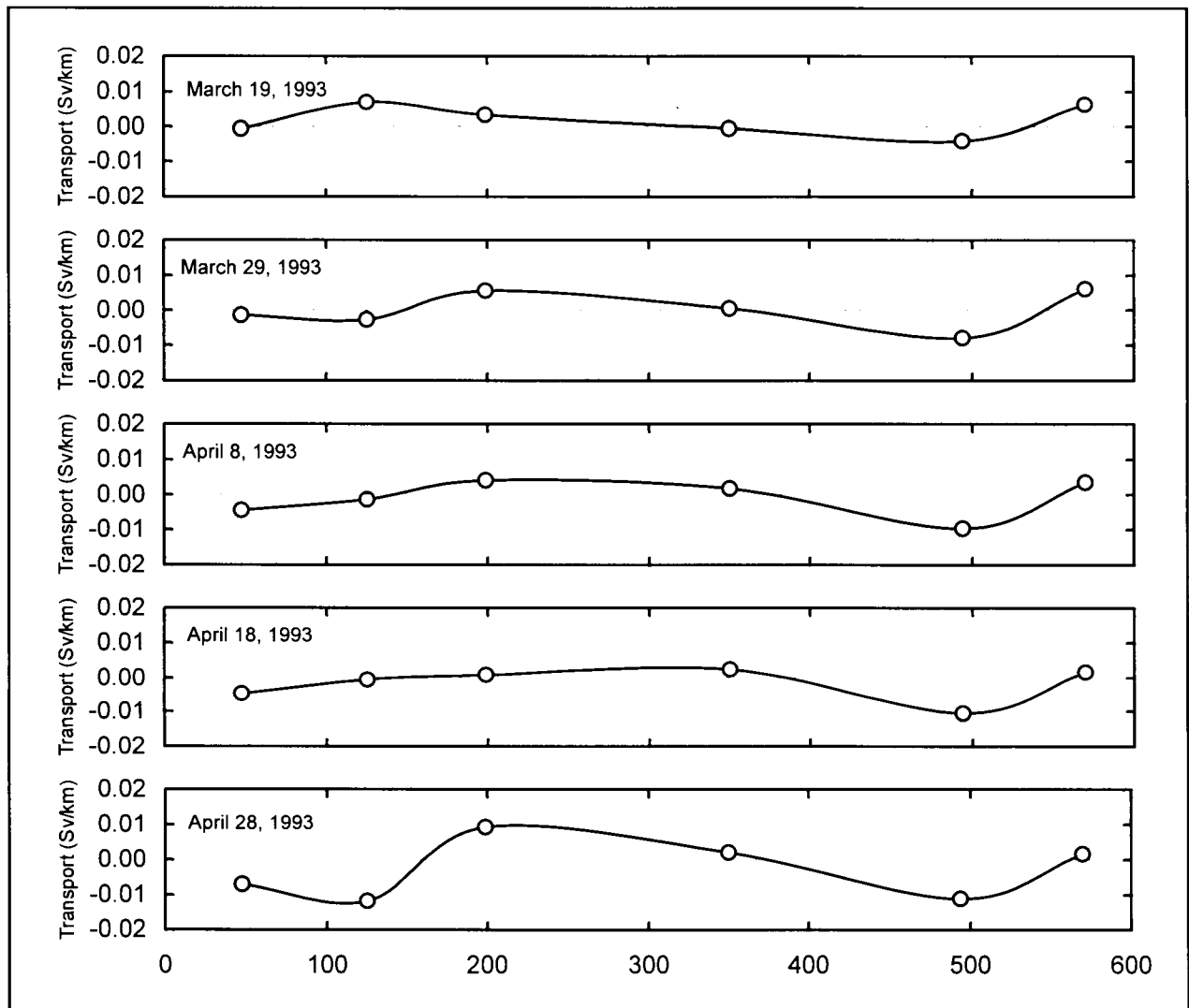


Figure B4. Estimated offshelf transport per km from March 19 – April 28, 1993, as a function of distance north and east along the 200-meter isobath from LATEX-A mooring 4. Circles represent locations half way between moorings 4, 6, 7, 8, 11, 13, and 48.

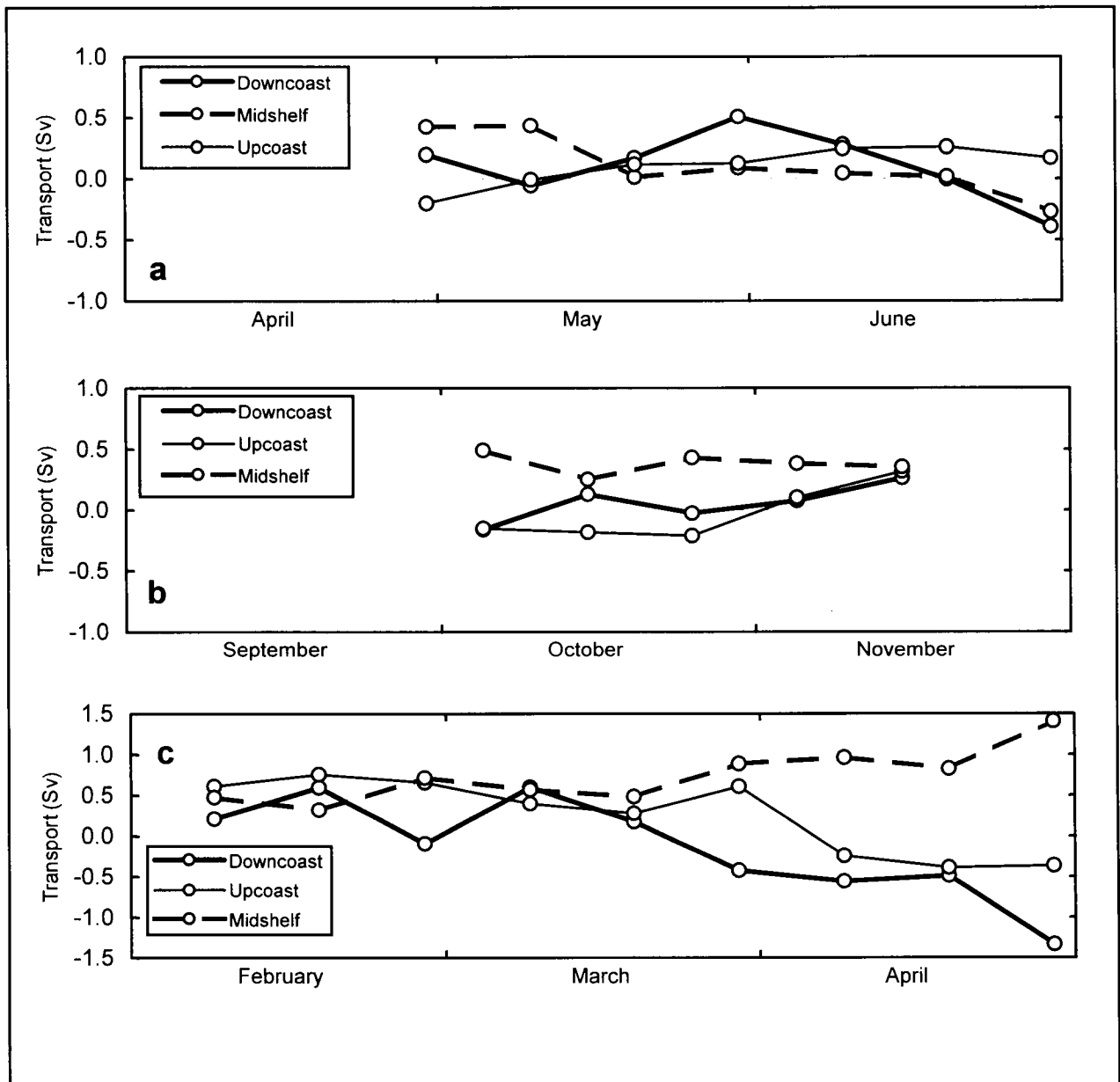


Figure B5. Estimated offshore geostrophic transport across the Louisiana-Texas shelf break by alongshore shelf region. (a) April 28 – June 27, 1992; (b) October 3 – November 12, 1992; and (c) February 7 – April 28, 1993. Notice the expanded transport scale in (c) required to illustrate the large offshore transport in midshelf and the large onshore transport in the downcoast region in late April 1993.



The Department of the Interior Mission

As the Nation's principal conservation agency, the Department of the Interior has responsibility for most of our nationally owned public lands and natural resources. This includes fostering sound use of our land and water resources; protecting our fish, wildlife, and biological diversity; preserving the environmental and cultural values of our national parks and historical places; and providing for the enjoyment of life through outdoor recreation. The Department assesses our energy and mineral resources and works to ensure that their development is in the best interests of all our people by encouraging stewardship and citizen participation in their care. The Department also has a major responsibility for American Indian reservation communities and for people who live in island territories under U.S. administration.



The Minerals Management Service Mission

As a bureau of the Department of the Interior, the Minerals Management Service's (MMS) primary responsibilities are to manage the mineral resources located on the Nation's Outer Continental Shelf (OCS), collect revenue from the Federal OCS and onshore Federal and Indian lands, and distribute those revenues.

Moreover, in working to meet its responsibilities, the **Offshore Minerals Management Program** administers the OCS competitive leasing program and oversees the safe and environmentally sound exploration and production of our Nation's offshore natural gas, oil and other mineral resources. The **MMS Royalty Management Program** meets its responsibilities by ensuring the efficient, timely and accurate collection and disbursement of revenue from mineral leasing and production due to Indian tribes and allottees, States and the U.S. Treasury.

The MMS strives to fulfill its responsibilities through the general guiding principles of: (1) being responsive to the public's concerns and interests by maintaining a dialogue with all potentially affected parties and (2) carrying out its programs with an emphasis on working to enhance the quality of life for all Americans by lending MMS assistance and expertise to economic development and environmental protection.